

**SIMULATION STUDY ON THE EFFECT OF FREQUENCY AND MEDIUM
RESISTIVITY ON THE PROPAGATION OF ELECTROMAGNETIC (EM)
WAVE**

By

MUHAMMAD FIDZRUL AZUAN BIN RAZALI

FINAL REPORT

Submitted to the Electrical & Electronics Engineering Programme
in Partial Fulfillment of the Requirements
for the Degree
Bachelor of Engineering (Hons)
(Electrical & Electronics Engineering)

Universiti Teknologi Petronas
Bandar Seri Iskandar
31750 Tronoh
Perak Darul Ridzuan

© Copyright 2011

by

Muhammad Fidzrul Azuan bin Razali, 2011

CERTIFICATION OF APPROVAL

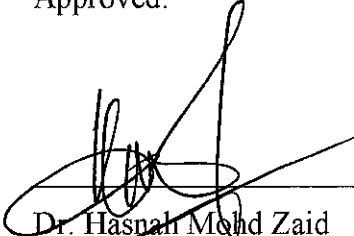
SIMULATION STUDY ON THE EFFECT OF FREQUENCY AND MEDIUM RESISTIVITY ON THE PROPAGATION OF ELECTROMAGNETIC (EM) WAVE

by

Muhammad Fidzrul Azuan bin Razali

A project dissertation submitted to the
Electrical & Electronics Engineering Programme
Universiti Teknologi PETRONAS
in partial fulfillment of the requirement for the
Bachelor of Engineering (Hons)
(Electrical & Electronics Engineering)

Approved:



Dr. Hasnali Mohd Zaid

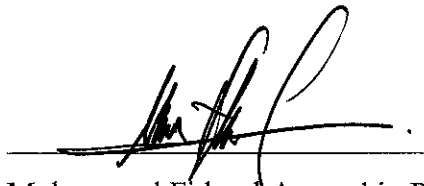
Project Supervisor

UNIVERSITI TEKNOLOGI PETRONAS
TRONOH, PERAK

MAY 2011

CERTIFICATION OF ORIGINALITY

This is to certify that I am responsible for the work submitted in this project, that the original work is my own except as specified in the references and acknowledgements, and that the original work contained here have not been undertaken or done by unspecified sources or persons.

A handwritten signature in black ink, consisting of stylized initials and a surname, written over a horizontal line.

Muhammad Fidzrul Azuan bin Razali

ABSTRACT

This project is to investigate the effect of frequency and resistive medium on the propagation of EM waves for application in Seabed Logging. Seabed Logging is an application of the marine controlled source electromagnetic (CSEM) method that is used to directly detect and characterize possible hydrocarbon-bearing prospects. The CSEM method has been used for a long time before, but the application as a direct hydrocarbon indicator is relatively new. The central idea of SBL is the guiding of electromagnetic energy in thin resistive layers within conductive sediments. Even though it has been well known for a long time that electromagnetic signals can propagate from a conductive region to another via resistive regions such as air or resistive parts of the lithosphere, its application in hydrocarbon exploration has not been developed until recently. [1] This might be due to the uncertainty of getting any significant response from thin resistive layers such as hydrocarbon reservoirs since electromagnetic energy is highly attenuated in conductive sediments. CST (Computer Simulation Technology) software will be used in this project to model an antenna and the EM waves. The parameters such as the EM wave's frequency and types of resistive medium used will represent the actual offshore environment. From the result of the simulation, it shows that different frequency will give different reading at the receiver. Lower frequency will give higher magnitude of B-Field at the receiver. And medium resistivity with higher resistivity will respond and reflect the EM energy to the receiver.

ACKNOWLEDGEMENTS

This research project would not have been possible without the support of many people. The author wishes to express his gratitude to his supervisor, Dr. Hasnah Mohd Zaid who was abundantly helpful and offered invaluable assistance, support and guidance. Special thanks also to all his friends, especially to Post-Graduate student, Azliza, Khairil, and Ridzuan for sharing the literature and invaluable assistance. The author would also like to convey thanks to the University of Technology Petronas for providing the research and laboratory facilities. The author wishes to express his love and gratitude to his beloved families for their understanding and endless love, through the duration of this project.

TABLE OF CONTENTS

ABSTRACT	iv
ACKNOWLEDGEMENTS	v
LIST OF TABLES	ix
LIST OF FIGURES	x
LIST OF ABBREVIATIONS	xii
CHAPTER 1: INTRODUCTION	1
1.1 Background of Study	1
1.2 Problem Statement	2
1.3 Objective	2
1.4 Scope of the Project	2
1.4.1 Relevancy of the Project	2
1.4.2 Feasibility of the Project within the Scope and Time Frame	3
CHAPTER 2: LITERATURE REVIEW	4
2.1 Hydrocarbon Detection Method	4
2.1.1 Seismic Method	4
2.1.2 Seabed Logging (SBL) Method	6
2.1.3 Progress and Issued in SBL	10
2.2 Electromagnetic Wave (EM)	11
2.2.1 EM Wave: Origin and Theory	11
2.2.2 Maxwell's Equation	12
2.2.3 Permeability, μ and Permittivity, ϵ	13

2.2.4	<i>Skin Depth, δ and Attenuation</i>	13
2.2.5	<i>Reflection and Refraction of EM wave</i>	14
2.3	Scale Model Calculation	16
2.4	Computer Simulation Technology (CST)	18
CHAPTER 3: PROJECT METHODOLOGY.		21
3.1	Project Activity Flow	21
3.2	Simulation Work	22
3.2.1	<i>Effect of Frequency and Medium Resistivity on the Propagation of EM waves</i>	22
3.2.2	<i>Application in SBL</i>	22
3.3	Simulation Structure	23
3.3.1	<i>Lab Scale Calculation</i>	23
CHAPTER 4: RESULT AND DISCUSSION		27
4.1	Simulation 1 – Effect of Different Frequency	27
4.2	Simulation 2 – Effect of Different Medium Resistivity	28
4.3	Simulation 3 – Effect of Different Frequency (Full scale)	29
4.4	Simulation 4 – Effect of Different Depth of Overburden (Full Scale)	32
4.5	Simulation 5 – Effect of Different Frequency (Lab Scale)	36
4.6	Simulation 6 – Effect of Different Depth of Overburden (Lab Scale)	40
4.7	Discussion	44
4.7.1	<i>Effect of Frequency and Medium Resistivity on Propagation of EM waves</i>	44
4.7.2	<i>Effect of EM Wave with Different Frequency in SBL</i>	45
4.7.3	<i>Effect of EM Wave with Different Depth of Overburden in SBL.</i>	46

CHAPTER 5: CONCLUSION AND RECOMMENDATION	47
5.1 Conclusion	47
5.2 Recommendation	48
REFERENCES	49
APPENDICES	52

LIST OF TABLES

Table 1: Maxwell's Macroscopic Equation	12
Table 2: Percentage, % Difference for Seafloor with Hydrocarbon and Without Hydrocarbon (Full Scale)	32
Table 3: Percentage, % Difference for Different Depth of Overburden (Full Scale)	36
Table 4: Percentage, % Difference for Seafloor with Hydrocarbon and Without Hydrocarbon (Lab Scale)	40S
Table 5: Percentage, % Difference for Different Depth of Overburden (Lab Scale)	44
Table 6: Gant Chart for FYP I	54
Table 7: Gant Chart for FYP II	55

LIST OF FIGURES

Figure 1: Application of Seismic Method in Ground-Water Exploration	4
Figure 2: Seismic 2D Data	5
Figure 3: Application of Different Resistivity in Seabed Logging	6
Figure 4: Schematic Diagram of Air-Water-Sediment Geometry and Receiver (Rx) Layout on Seabed	8
Figure 5: Third-generation Seabed-logging Receivers	9
Figure 6: Resistivity Map of Highlight Location of Resistive Anomalies	9
Figure 7: Diagram of Electromagnetic Waves	11
Figure 8: Reflection of EM Waves	14
Figure 9: Refraction of EM Waves	15
Figure 10: CST DS – Structure Design	19
Figure 11: CST DS – Data Retrieval	20
Figure 12: CST DS – 3D Result	20
Figure 13: Project Activity Flow	21
Figure 14: Structure Visualization – Layer Thickness	24
Figure 15: Structure Visualization – Survey Area	25
Figure 16: Structure Visualization – Distance of Transmitter to Receiver	26
Figure 17: Magnitude versus Offset, Sea Water ($\sigma = 3 \text{ S/m}$)	27
Figure 18: Magnitude versus Offset, Soil ($\sigma = 1.5 \text{ S/m}$)	28
Figure 19: Magnitude versus Offset, 0.78 MHz	28
Figure 20: Magnitude versus Offset, 0.125 Hz	29
Figure 21: Magnitude versus Offset, 0.25 Hz	30
Figure 22: Magnitude versus Offset, 0.5 Hz	30
Figure 23: Magnitude versus Offset, 1 Hz	30
Figure 24: Magnitude versus Offset, 0.125 Hz, 0.25 Hz, 0.5 Hz, 1 Hz	31
Figure 25: Magnitude versus Offset, Different Depth of Overburden at 0.125 Hz	33

Figure 26: Magnitude versus Offset, Different Depth of Overburden at 0.25 Hz	34
Figure 27: Magnitude versus Offset, Different Depth of Overburden at 0.5 Hz	34
Figure 28: Magnitude versus Offset, Different Depth of Overburden at 1 Hz	35
Figure 29: Magnitude versus Offset, 0.78 MHz	37
Figure 30: Magnitude versus Offset, 1.56 MHz	37
Figure 31: Magnitude versus Offset, 3.13 MHz	38
Figure 32: Magnitude versus Offset, 6.25 MHz	38
Figure 33: Magnitude versus Offset, 0.78 MHz, 1.56 MHz, 3.13 MHz, 6.25 MHz	39
Figure 34: Magnitude versus Offset, Different Depth of Overburden at 0.78 MHz	41
Figure 35: Magnitude versus Offset, Different Depth of Overburden at 1.56 MHz	42
Figure 36: Magnitude versus Offset, Different Depth of Overburden at 3.13 MHz	42
Figure 37: Magnitude versus Offset, Different Depth of Overburden at 6.25MHz	43

LIST OF ABBREVIATIONS

CSEM	Control Source Electromagnetic
CST DS	Computer Simulation Technology Design Studio
CST	Computer Simulation Technology
EM	Electromagnetic
EMGS	ElectroMagnetic GeoServices
MHz	Megahertz
MVO	Magnitude versus Offset
OHM	Offshore Hydrocarbon Mapping
SBL	Seabed Logging
TE	Transverse Electric
TM	Transverse Magnetic

CHAPTER 1

INTRODUCTION

This chapter discussed the background of study, problem statement, objective, and scope of the project (relevancy and feasibility of the project within the scope and time frame).

1.1 Background of Study

Detecting and assessing hydrocarbon reservoirs without the need to drill test wells is a major importance to the petroleum industry. Seismic methods have traditionally been used in this context, but the results can be ambiguous. Another approach is to use electromagnetic sounding methods that exploit the resistivity differences between a reservoir containing highly resistive hydrocarbons and one saturated with conductive saline fluids.

Modeling presented by Eidesmo et al. (2002) demonstrates that by using seabed logging (SBL), a special application of frequency domain controlled source electromagnetic (CSEM) sounding, [2] the existence or otherwise of hydrocarbon bearing layers can be determined and their lateral extent and boundaries can be quantified. Such information provides valuable complementary constraints on reservoir geometry and characteristics obtained by seismic surveying.

1.2 Problem Statement

EM antenna propagates the EM waves and detects the existence of hydrocarbon reservoir. For deep target exploration, there is a difficulty in detecting hydrocarbon due to attenuation of EM waves. The attenuation of EM waves depends on the wave's frequencies that are propagated from the EM antenna and the resistive medium that the waves need to go through. Thus, it is necessary to know the behavior of EM waves that propagate through the seafloor into the subsurface.

1.3 Objective

The objectives of the project are:

- a) To study the effect of frequency and medium resistivity on propagation of EM waves used in Seabed Logging (SBL) method, using CST software.
- b) To study the application of SBL method using simulation.

1.4 Scope of the Project

The scope of study will involve the study of SBL method, and the application of CST software which is used to simulate EM waves. This project will involve the study on the effect of different frequencies, and the attenuation of EM waves when they pass through different mediums and the behavior of reflected waves using simulation.

1.4.1 Relevancy of the Project

PETRONAS is engaged with a lot of petroleum activities including upstream exploration and downstream oil refining. New technology is needed to explore oil and gas effectively. Universiti Teknologi Petronas (UTP) has discovered this new technology for Oil and Gas research and

development under the Fundamental & Applied Sciences Department (FASD), in line with PETRONAS's hydrocarbon detection project.

1.4.2 Feasibility of the Project within the Scope and Time Frame

During the first semester of Final Year Project (FYP 1), the target of this project is to be able to determine the effect of wave frequency and resistivity of medium on the propagation of EM waves by performing simulation using CST software. In semester 2 (FYP 2), the simulation will be upgraded by adding layers that represents the actual environment such as soil, sand, and hydrocarbon.

CHAPTER 2

LITERATURE REVIEW

This chapter discussed the various hydrocarbon detection methods and elaborates the concepts of the methods. It also explains the concepts of electromagnetic waves and CST simulation software.

2.1 Hydrocarbon Detection Method

2.1.1 Seismic Method

The conventional method used for oil and gas exploration is the seismic method. This method uses a controlled seismic source of energy such as a specialized air-gun or a seismic vibrator. The application of this method is shown in Figure 1.

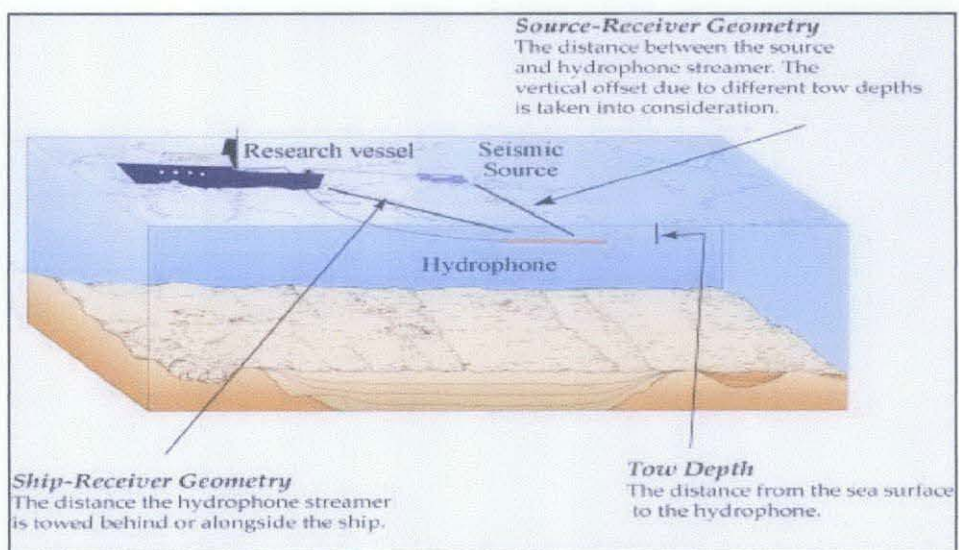


Figure 1: Application of Seismic Method in Ground-Water Exploration[3]

In seismic method, a sound source such as air-gun will be towed along the survey line by a ship. The acoustic energy will be reflected back to the receiver (hydrophone or array hydrophone) with different acoustic impedances. At the receiver, data will be converted into an analog signal which will be digitized and displayed with high-speed computers. The data then is interpreted by mapping it into computer programs.[3] An example of seismic data is shown in Figure 2.

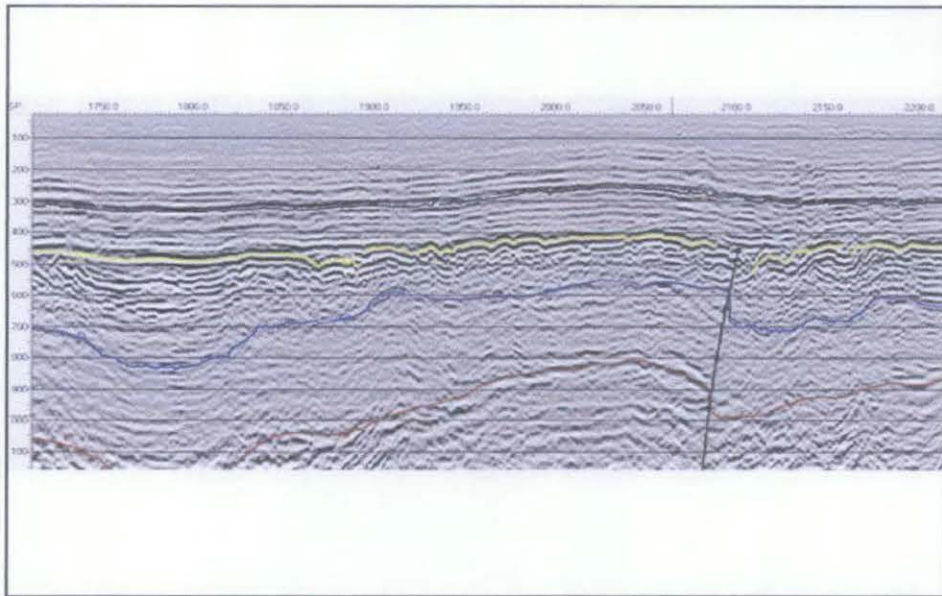


Figure 2: Seismic 2D Data[3]

Seismic sources use a variety of transmitters that differ in operating frequency. For example, an air-gun operates at 100-1500 Hz. Other type of transmitters such as Sparker operates at 50-4000 Hz. By using higher frequency, it can provide higher resolution, but lower penetration. Lower frequency will give higher penetration but less resolution.[4]

Seismic method depends on the elastic properties and the density of the structures. It will be useful to differentiate between boundaries that have different densities.[5] It is possible to estimate the depth of the structure that is generated by the reflection because of the time taken for a reflection to be received by the receiver. This can rapidly overwhelm the collected data. [6] This approach also involves massive investment

because the equipment in general is more expensive than the equipment required for other geophysical surveys. Since this method is unable to determine whether the liquid found below the seabed is hydrocarbon or not, a drill test needs to be done. Thus, it will cause a lot of wasted cost if there is no hydrocarbon found.

2.1.2 Seabed Logging (SBL) Method

The seabed logging (SBL) method is a remote resistivity sensing method and exploit the fact that hydrocarbons are electric insulators and, the hydrocarbons filled in the reservoirs normally are more resistive than the surrounding water-filled sediments. The resistivity of the reservoirs will normally vary depending on the fluid composition (the degree of hydrocarbon saturation). [7]

Over the years, seabed logging has become a new method to reduce drilling risk. One of the advantages of this method is, the electrical resistivity of a formation is determined primarily by the fluid. Hydrocarbon that contains rocks show significantly higher resistivity than water that contains the same rocks. The concept of SBL method is shown in Figure 3.

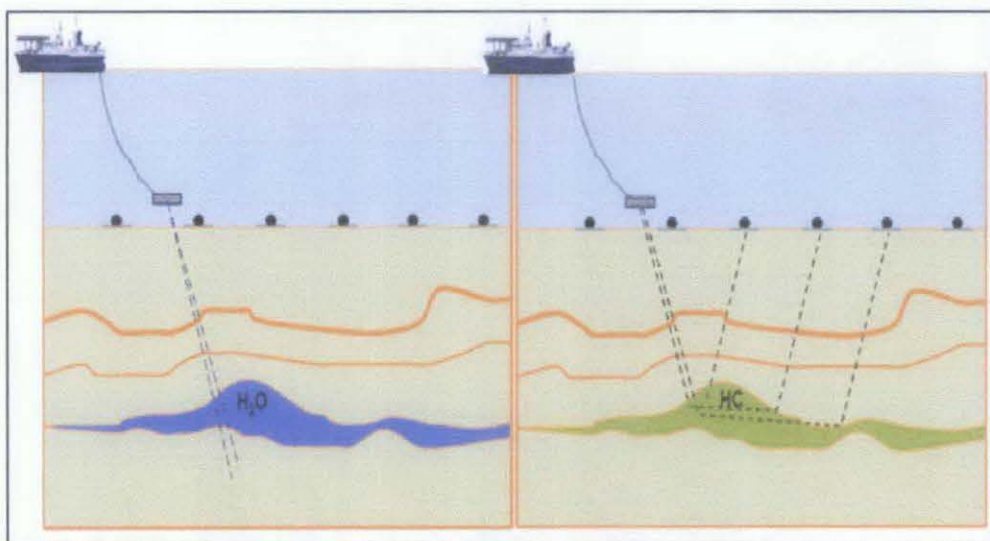


Figure 3: Application of Different Resistivity in Seabed Logging[7]

EM waves have two important components which are the transverse electric (TE) and transverse magnetic (TM) modes. These two modes respond differently to a resistive layer (hydrocarbon-filled reservoir). The TM mode will penetrate into the layer through a narrow aperture of angle of incidents, where the reflection coefficient is small. The TM mode will be trapped inside the layer and propagate with higher speed and relatively low attenuation throughout the resistive layer. The energy leaks out on the way as seismic refraction. [8]

The good thing about TM mode is the low attenuation of the wave which is important in order to get higher reading by the receiver. The low attenuation of the TM mode inside reservoirs is due to the high resistivity (low conductivity) of reservoir that hinders the current from flowing vertically between the top and base of the reservoir. At the reservoir boundaries, or at “holes” in the reservoir, the current again will flow as normal, and together with internal reflection from edges, a new anomaly will appear on the surface as “edge effects”. These effects may be used to determine reservoir boundaries. [9]

The tendency for resistive layers in the sea surface to guide low-frequency EM energy has made CSEM technique becomes very unique. The low-frequency EM energy will be guided from a receiver at intermediate and long offsets. EM energy that propagates in conductive beds such as overburden will be rapidly attenuated. Comparing to seismic wave, the velocity of propagation varies greatly between the resistive and conductive layers. The energy in the subsurface may be attenuated and weakened due to resistive layer of the structure in the sea, however at higher resistive contrast, it will be reflected and refracted back. The energy will be guided along the reservoir, going through the resistive structures with low attenuation and much higher velocity. This is the path for low-frequency EM energy to be emitted by a transmitter and reached a receiver several kilometers distant. [10] The schematic diagram of the path is shown in Figure 4.

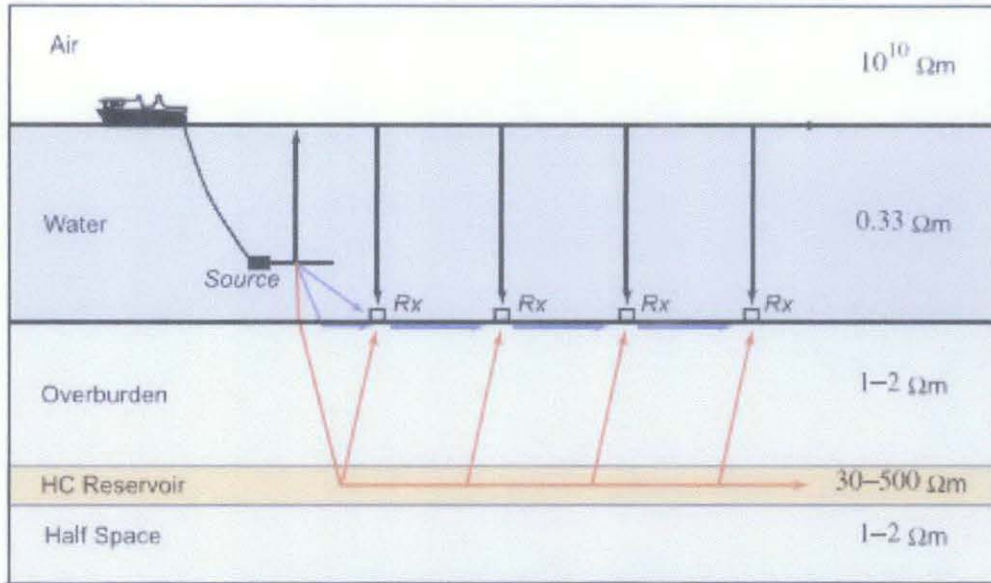


Figure 4: Schematic Diagram of Air-Water-Sediment Geometry and Receiver (Rx) Layout on Seabed[9]

Black arrows denote refracted transmission of electromagnetic signals via the airwater interface. Blue arrows denote direct transmission of electromagnetic signals through water and by refraction along the seabed. Red arrows denote refracted transmission of electromagnetic signals via a buried high-resistivity layer (hydrocarbon reservoir).[9] The receivers on the seabed will record the data or the energy reflected by the seabeds. From the data, we can detect whether the seabeds contain the hydrocarbon or not by the energy that is given off. The presence of the hydrocarbon reservoirs can be analyzed by looking at the difference in the energy which is the difference in resistivity of the seabeds. The thickness and the resistivity of the layers will affect the reading of signal received by the receiver on the surface. The signal will be higher for shallow reservoirs because of the close distance between the source and the receiver. [11] The receiver used by EMGS is as shown in Figure 5.



Figure 5: Third-generation Seabed-logging Receivers[11]

During a survey, the receiver will be dropped onto the seabed under the weight of concrete anchors. When all the receivers are in position, the towfish is pulled along the survey line. Data is recorded in the datalogger section of each receiver.[12]

The result of the survey will be displayed as EM magnitude versus offset (MVO). Summary plots on seabed maps as shown in Figure 6 is the survey results and the prospect outline.

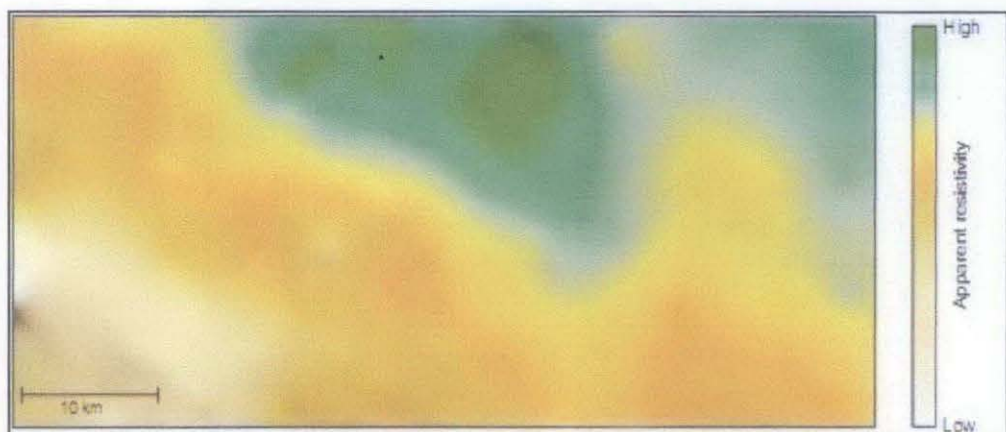


Figure 6: Resistivity Map of Highlight Location of Resistive Anomalies[11]

2.1.3 Progress and Issued in SBL

Seabed logging has been tested and showed good result in two hydrocarbon provinces, which is off West Africa in 2003 and in the Norwegian Sea in 2001. The test was demonstrated by using scientific oceanographic marine CSEM equipment. [7] This survey geometry was planned to optimize the response of energy guided through hydrocarbon-bearing formations. Data from the survey was recorded with equipment supplied by several research centers (USA and UK).

In October 2001, Statoil techniques were tested and recorded for Statoil, Shell, and Enterprise Oil in the North Sea. This event was done as a commercial concept. The test came out with very accurate and encouraging result, and since then, many companies have used seabed-logging data. [10]

ElectroMagnetic GeoServices ASA (EMGS) is a Norway-based company also one of the active company that provide services using seabed logging. The company offer services within both 2D and 3D mapping of hydrocarbon reservoirs for oil and gas companies. Latest news in February 2011, the company has made a water-depth record by towing an EM source at a depth of 3449 m. This survey is conducted as part of the work they are performing for PEMEX in the Gulf of Mexico. [13]

In SBL, there is an issue regarding the resistivity of subsurface in shallow water. In 2008, a survey has been done in Malaysia by PETRONAS researcher regarding shallow water exploration. The subsurface resistivity has been considered difficult to interperate because of the strong effects from the reflection of EM waves from the sea-surface, also known as airwave. The airwave masks all the response from the subsurface. To overcome this problem, they use many kind of interpretation tools including attribute analysis and inversion. [14]

2.2 Electromagnetic Wave (EM)

2.2.1 EM Waves: Origin and Theory

Electromagnetic waves were first postulated by James Clerk Maxwell and subsequently confirmed by Heinrich Hertz. Maxwell derived a wave form of the electric and magnetic equations, revealing the wave-like nature of electric and magnetic fields, and their symmetry. Because the speed of EM waves predicted by the wave equation coincided with the measured speed of light, Maxwell concluded that light itself is an EM wave.[15] Figure 7 shows the behaviour of EM waves.

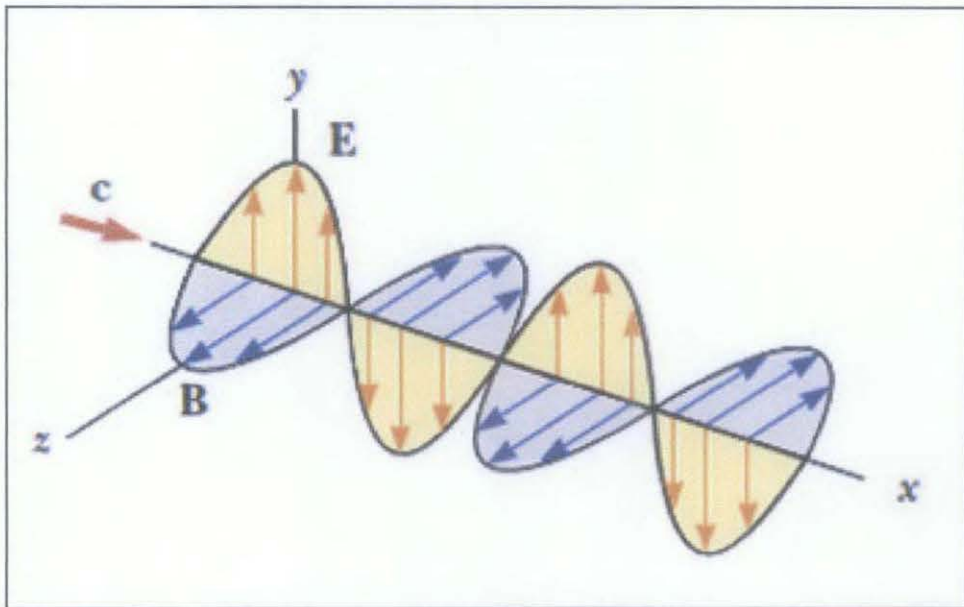


Figure 7: Diagram of Electromagnetic Waves[15]

Electromagnetic radiation is a phenomenon that takes the form of self-propagating waves in a vacuum or in matter. It comprises electric and magnetic field components, which oscillate in phase perpendicular to each other and perpendicular to the direction of energy propagation. According to Maxwell's extension of ampere's law, a changing electric field (according to Faraday's Law), creating a self-supporting oscillation in the field that moves at the speed of light. This wave will propagate through the resistive medium in the sea which is soil,

sand and sea water and will communicate/reflected back to the sea surface after interaction with hydrocarbon because of its high resistivity.

2.2.2 Maxwell's Equations

In 1864, Maxwell published the theory which is expressed as Maxwell equations developed from mathematical theory for electromagnetism. The famous Maxwell's equations are Gauss's Law, Gauss's Law for Magnetism, Faraday's Law, and Ampere's Law with Maxwell's correction, as shown in Table 1. Gauss's law describes the relationship between an electric field and the generating electric charges while Gauss' law for magnetism explains more on magnetic field due to material is generated by a configuration called a dipole. Magnetic dipoles are best explained as a current that never begins nor ends but loops or extends to infinity and back.

Table 1: Maxwell's Macroscopic Equation

Name	Formula
Gauss's law	$\nabla \cdot E = \frac{\rho}{\epsilon}$
Gauss's law for magnetism	$\nabla \cdot B = 0$
Maxwell-Faraday equation (Faraday's law of induction)	$\nabla \times E = -\frac{\delta B}{\delta t}$
Ampere's circuital law (with Maxwell's correction)	$\nabla \times B = \mu J + \mu\epsilon \frac{\delta E}{\delta t}$

The reason why electromagnetic waves travel through space constantly is explained from the last equation which is Ampere's law with Maxwell's correction. Original Ampere's law stated that magnetic field can be generated by electrical current. But, Maxwell has proved that magnetic field can also be generated by changing of electric fields. These equations allow self-sustaining of electromagnetic waves.

2.2.3 Permeability, μ and Permittivity, ϵ

Basically, we can express permeability, μ as the measure of the ability of a material to support the formation of a magnetic field within itself. In other words, it is a degree of magnetization that material obtains in response to an applied magnetic field.[16] Permittivity, ϵ is define as a measure of how an electric field affects, and is affected by dielectric medium.[17] Permittivity, ϵ and permeability, μ look similar since permittivity refers to ‘electrical phenomena’ and permeability refers to ‘magnetic field’. Basic concept of these measurement is important in order to understand the effect of EM wave when it goes through different medium with different value of permittivity and permeability.

2.2.4 Skin Depth, δ and Attenuation

The equation for skin depth is given as:

$$\delta = \sqrt{\frac{2}{\mu\sigma\omega}} \quad (1)$$

Where μ is the permeability of free space, ω is the angular frequency of the electromagnetic wave signal, and σ is the conductivity of medium in which the EM wave propagates. Skin depth is defined as the distance of the EM wave is able to penetrate into the medium it goes through. From the equation, the skin depth is large for high resistivity medium and less attenuation compared to low resistivity medium. This is because, in shorter skin depth or low resistivity medium, the response of electric and magnetic field will decreased. Thus, low frequency is used to get less attenuation and to increase the response of electric and magnetic field. [18]

2.2.5 Reflection and Refraction of EM wave

Reflection is the phenomena when the wave front changes direction at an interface between two different media, in the way that the wave front returns into the medium from which it originated. As shown in Figure 8, the physical law of reflection of electromagnetic wave is the angle of reflection equals the angle of incidence, and we measure these angles to the normal-vector of the surface, namely the two angles α and β are equal.[19]

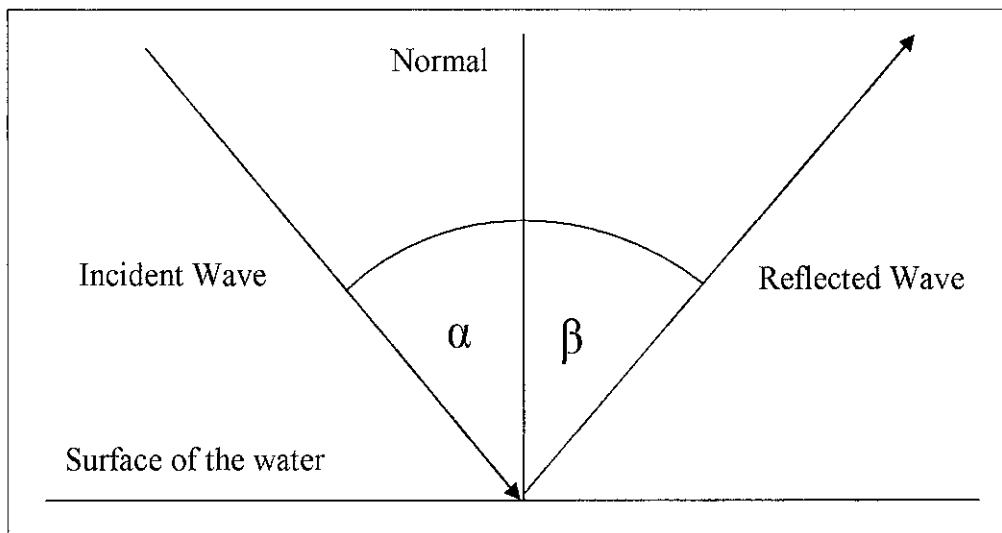


Figure 8: Reflection of EM Waves

Snell's law describes the relationship between the angle of incidence and refraction: the ratio between them is a constant depending on the media or more exactly the ratio of the sines of the angles equals the ration of velocities in the two media.

$$\frac{\sin \theta_1}{\sin \theta_2} = \frac{v_1}{v_2} = \frac{n_2}{n_1} \quad (2)$$

or

$$n_1 \sin \theta_1 = n_2 \sin \theta_2 \quad (3)$$

According to this law, the direction of the wave can be refracted towards or from the normal line as shown in Figure 9.[19]

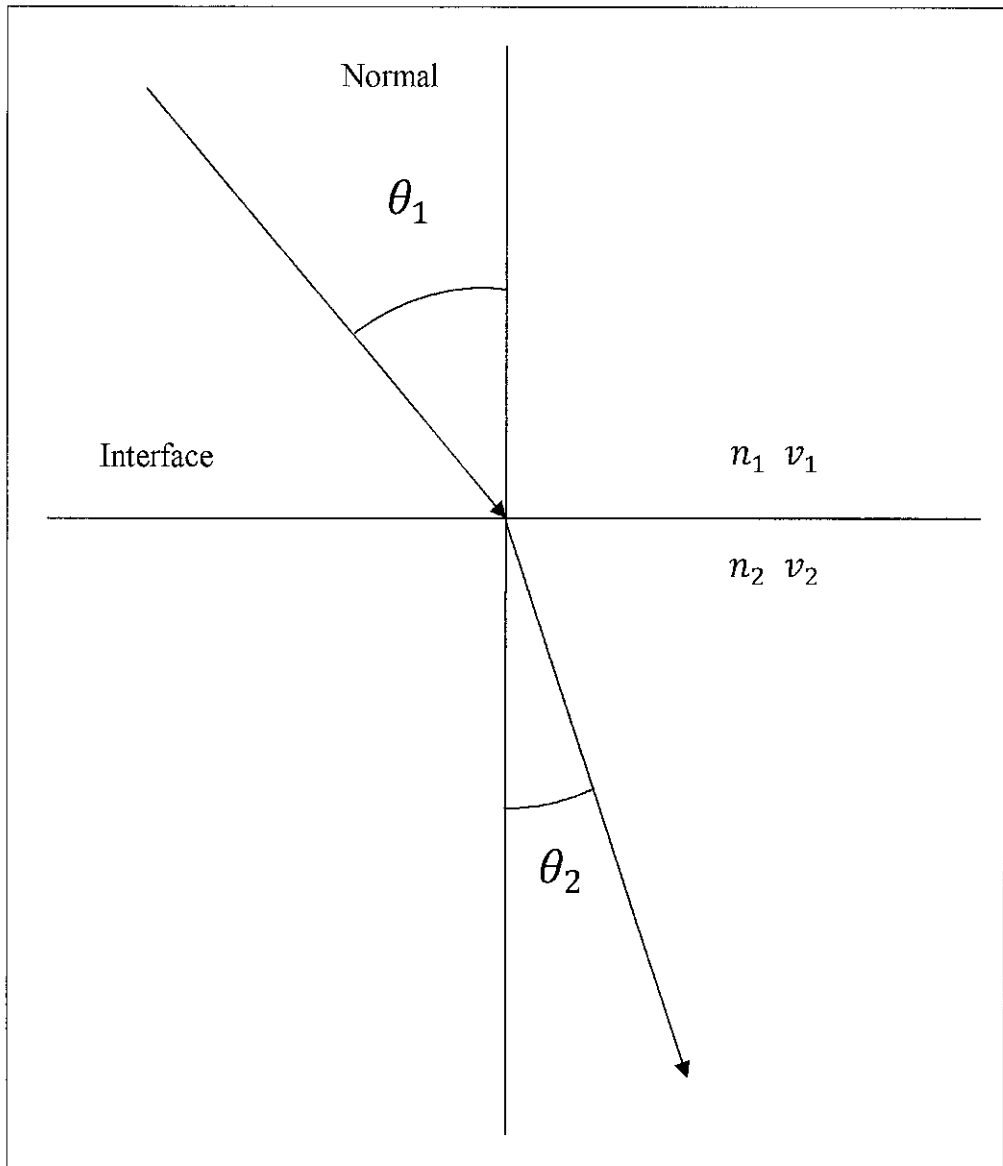


Figure 9: Refraction of EM Waves

When wave crosses a boundary between materials with different conductivity, it will be refracted. But, if the angle to the normal increased, the fraction of the wave will be decreased, until it reach the angle when total internal reflection occur. The wave will stop crossing the boundary and instead will be totally reflected back.

2.3 Scale Model Calculation

For experiment in the lab, a tank will be used to replicate the real seabed environment. Therefore a scale model calculation needs to be done. The ratio of the full scale and the lab scale dimensions is:

$$\frac{d_{fs}}{d_{lab}} = n \quad (4)$$

If

$$\left(\frac{\rho}{\mu f}\right)_{fs} = n^2 \left(\frac{\rho}{\mu f}\right)_{lab} \quad (5)$$

The full scale and the laboratory scale both generally concerned with nonmagnetic conductors $\mu = \mu_o$ the permeability of the free space, so that

$$\left(\frac{\rho}{f}\right)_{fs} = n^2 \left(\frac{\rho}{f}\right)_{lab} \quad (6)$$

for the frequency

$$\left(\frac{1}{f}\right)_{fs} = n^2 \left(\frac{1}{f}\right)_{lab} \quad (7)$$

$$\boxed{n^2 f_{fs} = f_{lab}} \quad (8)$$

If the scale factor is $n = 1500$

a) Wave length

If full scale frequency is 0.1 Hz

$$(1500)^2 (0.1 \text{ Hz}) = f_{lab}$$

$$225 \text{ KHz} = f_{lab}$$

$$\lambda = 2\pi \sqrt{\frac{2}{\mu\sigma\omega}}$$

$$\lambda = \sqrt{\frac{8\pi^2}{\mu\sigma\omega}}$$

$$\lambda = \sqrt{\frac{1}{10^{-7}\sigma f}}$$

For sea water conductivity is $\sigma = 5.2$

$$\begin{aligned}\lambda &= \sqrt{\frac{1}{10^{-7} \times 5.2 \times 225 \times 10^3}} \\ &= 2.92m\end{aligned}$$

b) Skin Depth

If full scale frequency is 0.1 Hz

$$(1500)^2 (0.1\text{Hz}) = f_{tab}$$

$$225\text{KHz} = f_{tab}$$

$$\delta = \sqrt{\frac{2}{\mu\sigma\omega}}$$

$$\delta = \sqrt{\frac{1}{4\pi^2 \times 10^{-7} \sigma f}}$$

For sea water conductivity is $\sigma = 5.2$

$$\begin{aligned}\delta &= \sqrt{\frac{1}{4\pi^2 \times 10^{-7} \times 5.2 \times 225 \times 10^3}} \\ &= 0.46m\end{aligned}$$

c) Phase Velocity

If full scale frequency is 0.1 Hz

$$(1500)^2 (0.1\text{Hz}) = f_{lab}$$

$$225\text{KHz} = f_{lab}$$

$$C_p = \sqrt{\frac{2\omega}{\mu\sigma}}$$

$$C_p = \sqrt{\frac{10^7 \times f}{\sigma}}$$

For sea water conductivity is $\sigma = 5.2$

$$C_p = \sqrt{\frac{10^7 \times 225 \times 10^3}{5.2}}$$

$$= 1.50 \times 10^6 \text{ m/s}$$

The simulation will be done in two dimensions which is full scale and lab scale dimensions. For full scale dimension, we used realistic distances apply in real SBL survey. Then, the scale will be reduced to perform lab scale simulation by using specific scale factor that can be done using calculation.

2.4 Computer Simulation Technology (CST)

CST is a software that can simulate static and low frequency of electromagnetic devices. Nowadays, many company such as EMGS and OHM had used CST to do simulation before starting to conduct a survey under the sea. CST become a powerfull tool to create a real environment on the seabed by considering an important parameters such as thermal, density, permeability and also permittivity of the structure under the seabed. Figure 10 shows the structure of CST software.

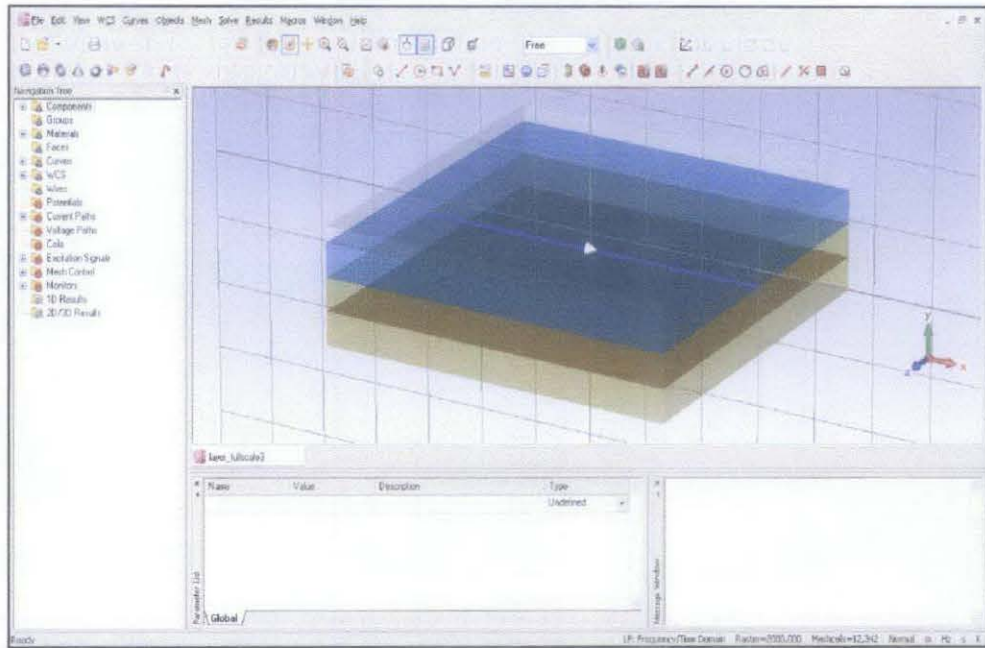


Figure 10: CST DS – Structure Design

In this research, we'll be using one of the CST's product which is CST Design Studio (CST DS), that can speed-up analysis of complex structure of electromagnetics systems. As we can see from Figure 10, an antenna and a receiver has been created inside the environment of the seabed which we can divide it layer by layer. The advantages of using CST DS is we can create the transmitter or antenna easily since there are many types of shapes provided in this software. Design of antenna also important in order to get a good transmitting EM wave. Figure 11 shows the retrieval data from the simulation.

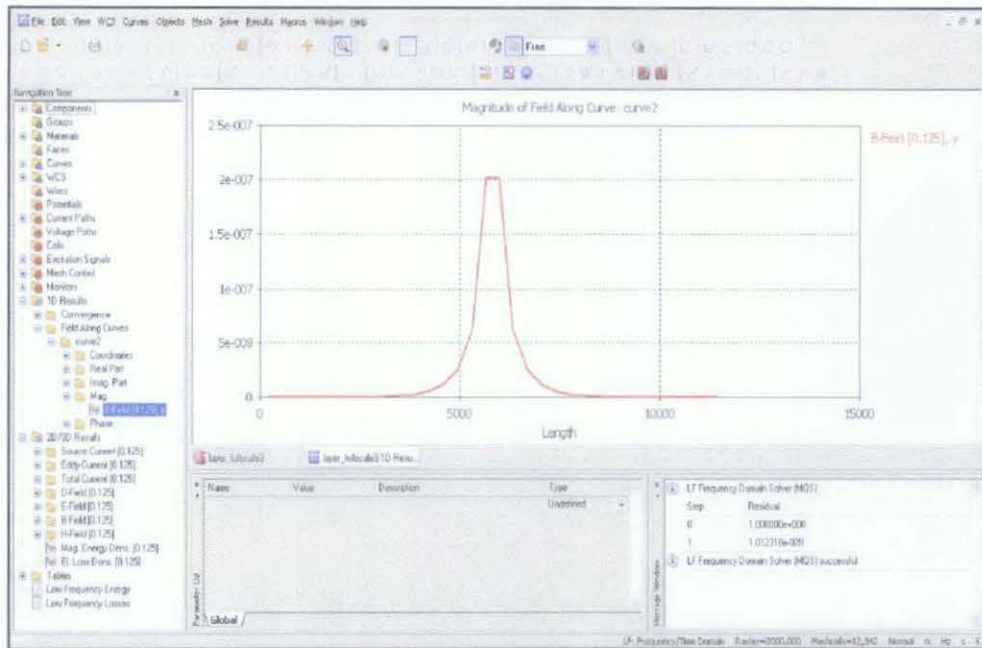


Figure 11: CST DS – Data Retrieval

CST DS will provide us with 1D and 2D/3D result. From Figure 11, is a 1D result that show the reading of data at the receiver. This data can easily be converted into excell file for further study. While in Figure 12, is 2D/3D result which showed us the intensity of B-Field in the environment that we had designed.

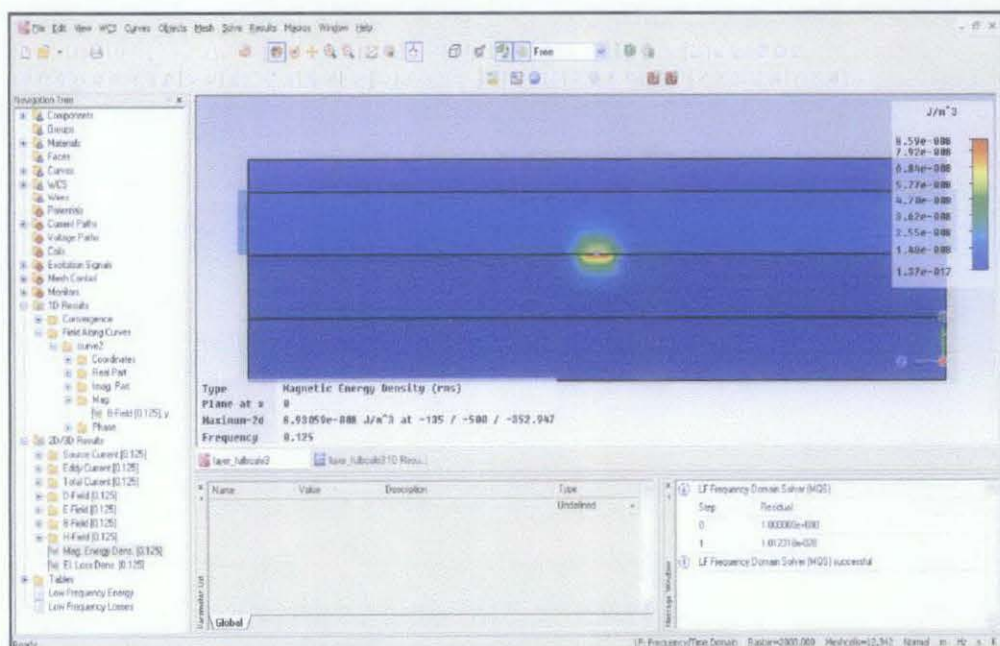


Figure 12: CST DS – 3D Result

CHAPTER 3

PROJECT METHODOLOGY

This chapter discussed on the activity flow of the project and explains on the simulation work that has been done.

3.1 Project Activity Flow

The flow of activity for the project is shown in Figure 13.

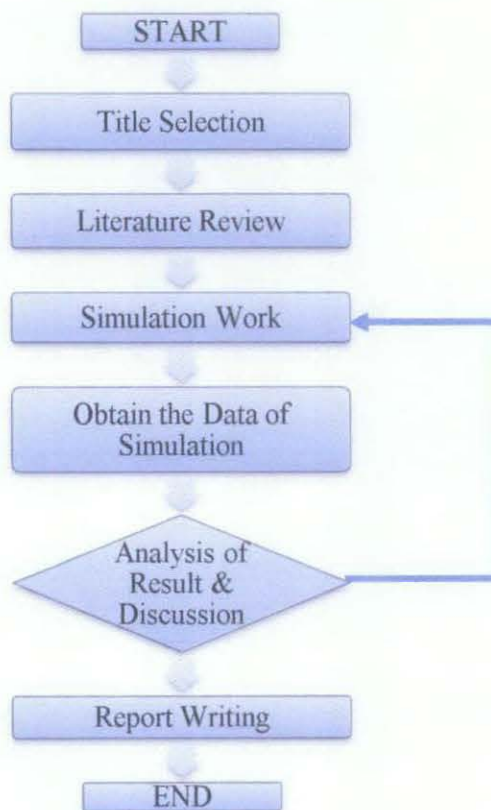


Figure 13: Project Activity Flow

3.2 Simulation Work

3.2.1 *Effect of Frequency and Medium Resistivity on the Propagation of EM waves*

During FYP 1, the simulation was done by investigating the propagation of EM wave in separated medium resistivity with different frequency.

- a) Simulation 1 – Effect of Different Frequency
- b) Simulation 2 – Effect of Different Medium Resistivity

3.2.2 *Application in SBL*

During FYP 2, a layer structure has been created, combining all the medium resistivity to make a real environment of the seabed. The effects on the EM energy that is reflected from resistive layer were investigated by manipulating the frequency of the EM source and the thickness of the overburden. The frequency we used in this simulation is from 0.125 Hz to 1 Hz for full scale dimension. Meanwhile for lab scale dimension, we used frequency from 0.78 MHz to 6.25 MHz. Then, we vary the depth of the overburden from 400 m for full scale and from 16 cm for lab scale, up until the receiver can no longer read the EM energy.

- a) Simulation 3 – Effect of Different Frequency (Full scale)
- b) Simulation 4 – Effect of Different Depth of Overburden (Full scale)
- c) Simulation 5 – Effect of Different Frequency (Lab scale)
- d) Simulation 6 – Effect of Different Depth of Overburden (Lab scale)

3.3 Simulation Structure

Real environment of the seabed such as sea water, overburden, under burden and others features can be designed and simulated using CST. We can put details for each feature such as conductivity, permittivity and also permeability. Accurate simulation design will provide a good result, thus guide us to better understanding on how the EM energy works in seabed-logging.

3.3.1 Lab Scale Calculation

For lab scale design, the scale factor will be, $n = 2000 - 3000$. But the scale factor can be higher than that since it is calculated based on the ratio between full scale and lab scale dimension that we used. For this simulation, we choose $n = 2500$ as our scaled factor and we will focus on the pattern of data between full scale and lab scale design.

Hence, our frequencies used in the lab scale's simulation are:

$$n^2 f_{fs} = f_{lab}$$

$$(2500)^2(0.125 \text{ Hz}) = 0.78 \text{ MHz}$$

$$(2500)^2(0.25 \text{ Hz}) = 1.56 \text{ MHz}$$

$$(2500)^2(0.5 \text{ Hz}) = 3.13 \text{ MHz}$$

$$(2500)^2(1 \text{ Hz}) = 6.25 \text{ MHz}$$

Figure 14, 15, and 16 show the full scale and lab scale of the simulation structure used in this simulation.

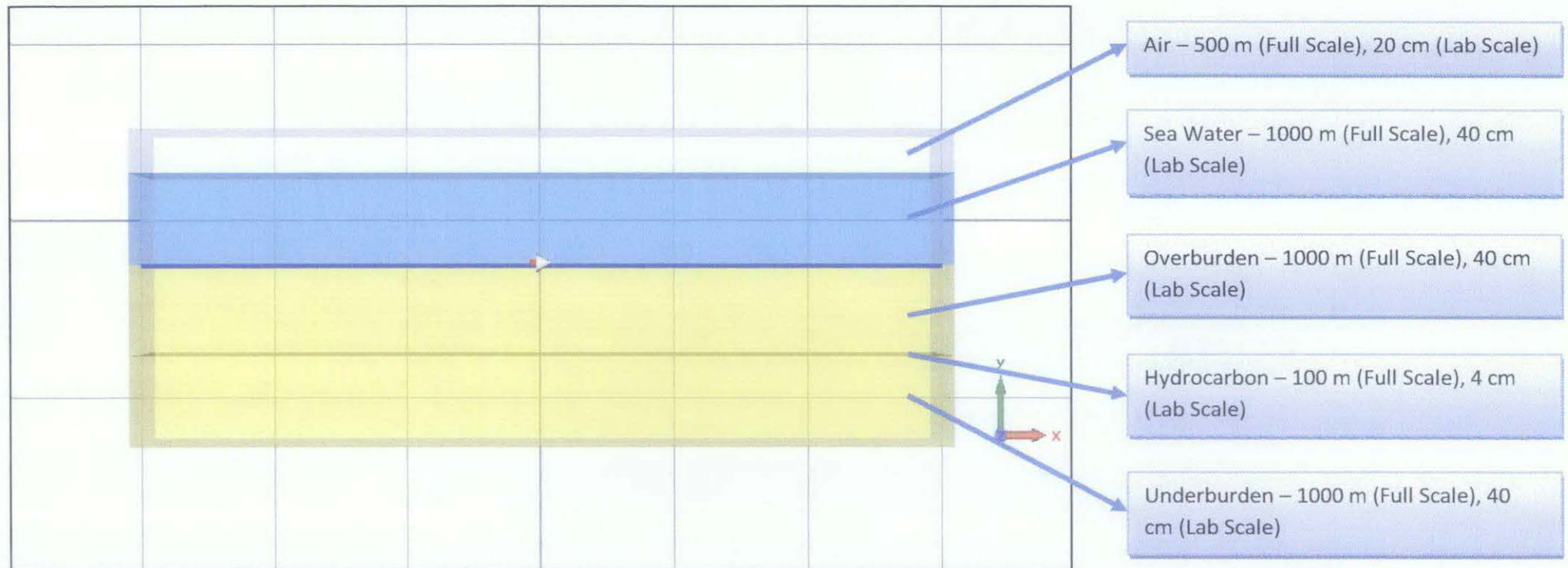


Figure 14: Structure Visualization – Layer Thickness

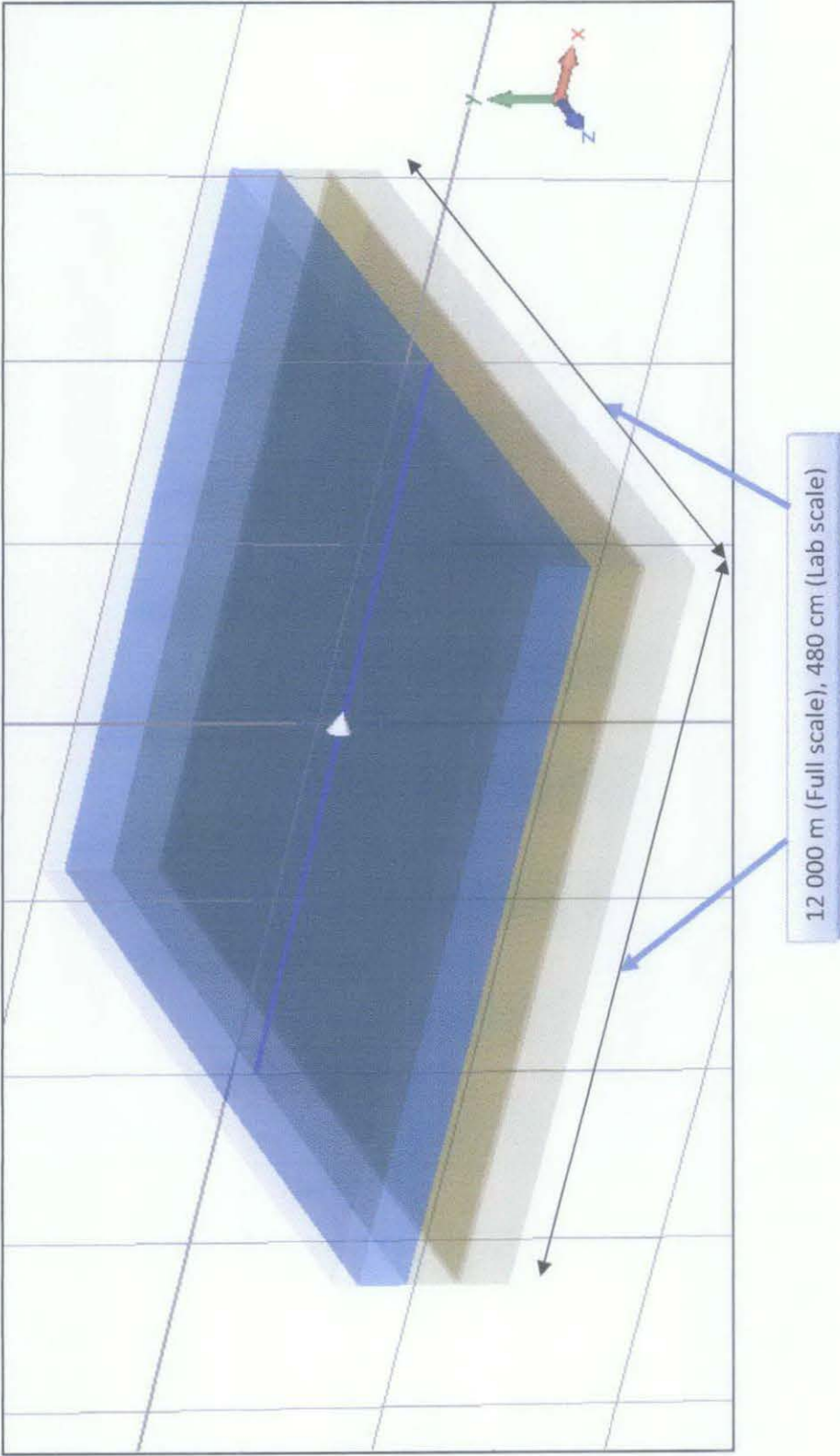


Figure 15: Structure Visualization – Survey Area

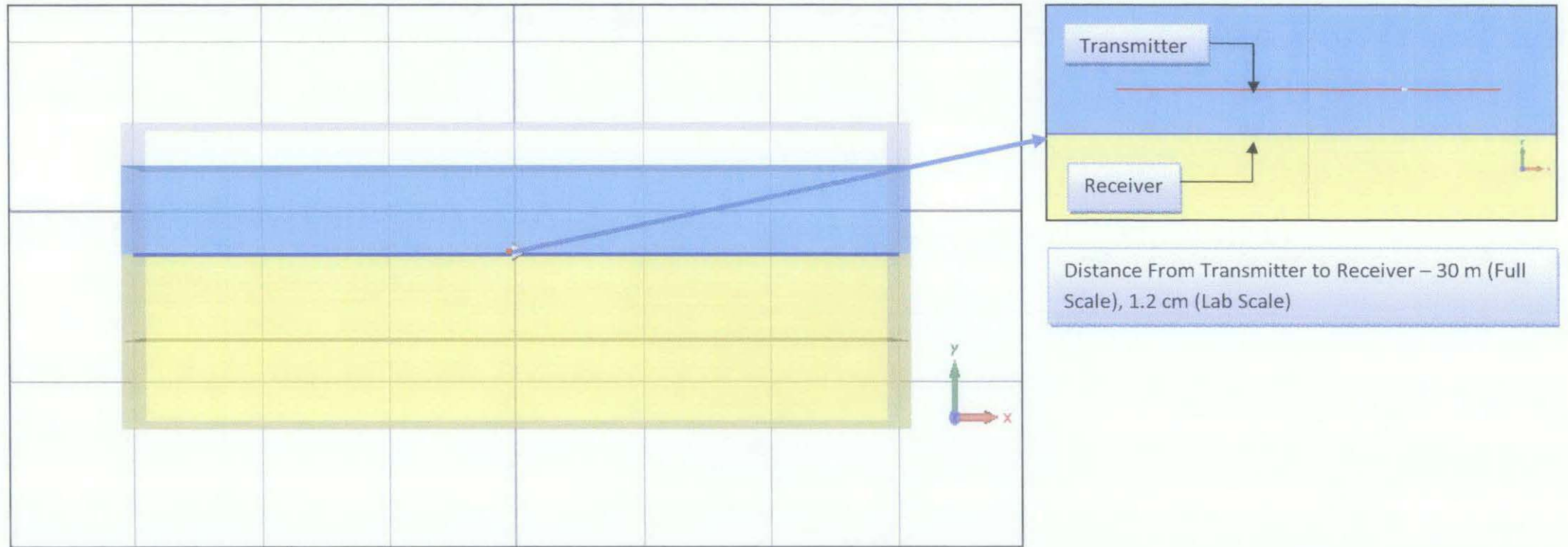


Figure 16: Structure Visualization – Distance of Transmitter to Receiver

CHAPTER 4

RESULT AND DISCUSSION

This chapter discussed the result of the simulations. The simulations were done for full scale and lab scale and the main objective is to see the effect of different frequency and medium resistivity on propagation of EM waves.

4.1 Simulation 1 – Effect of Different Frequency

For simulation 1, the objective is to see the effect of using different frequency of EM wave in only one medium of resistivity. Sea water and soil has been used as the medium resistivity.

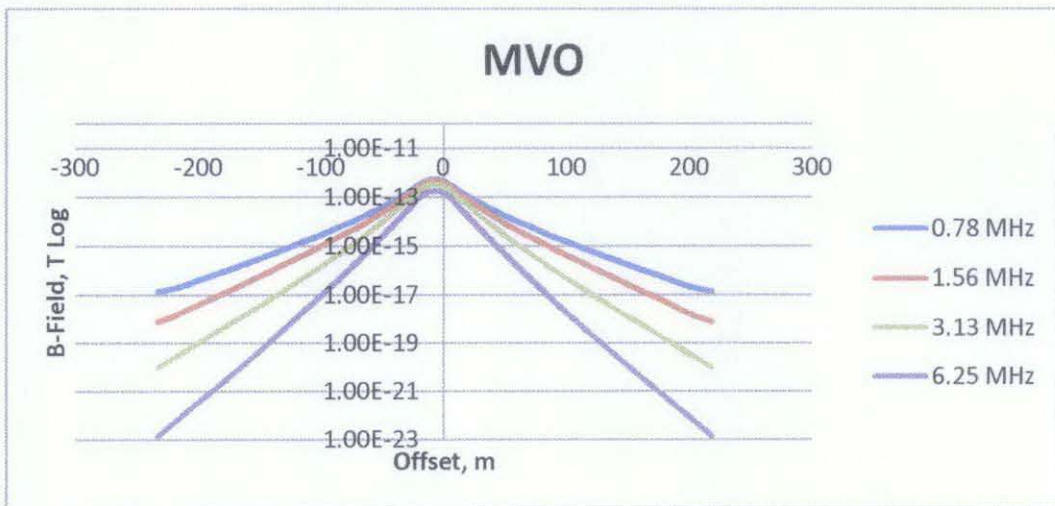


Figure 17: Magnitude versus Offset, Sea Water ($\sigma = 3 \text{ S/m}$)

From Figure 17, the lower frequency gives higher magnitude of B-Field compare to others. Same pattern of result is shown in Figure 18 (soil as medium). The difference between these two results is the magnitude of B-Field slightly higher for soil compared to magnitude of B-Field in sea

water. This is due to the conductivity of sea water which is higher than soil. Thus, sea water will cause more attenuation of EM energy.

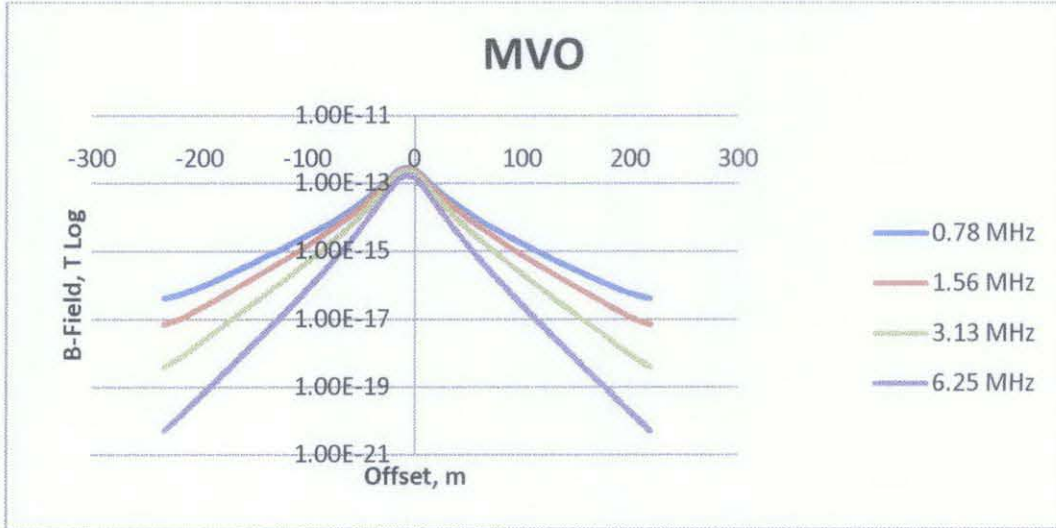


Figure 18: Magnitude versus Offset, Soil ($\sigma = 1.5 \text{ S/m}$)

4.2 Simulation 2 – Effect of Different Medium Resistivity

For simulation 2, the frequency used is constant, which is 0.78 MHz, and we used three types of medium resistivity which is sea water, air, and soil.

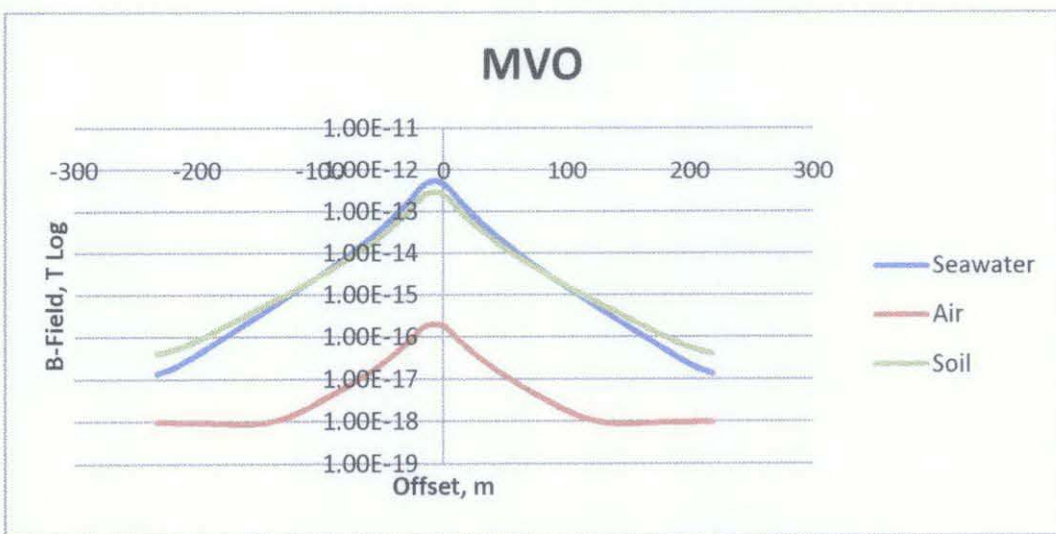


Figure 19: Magnitude versus Offset, 0.78 MHz

From Figure 19, the magnitude of B-Field is higher for soil, followed by sea water and air. This is due to different resistivity and conductivity of the medium resistivity. Sea water has the highest conductivity which is 3 S/m . Thus, EM waves will be attenuated more in sea water.

4.3 Simulation 3 – Effect of Different Frequency (Full scale)

In simulation 3, we want to study on the effect of different frequency on propagation of EM waves using real environment of the seabed structure. The simulation result will show us the magnitude of B-Field for the seabed that contains hydrocarbon with the one that are not. In Figure 20, the frequency used is 0.125 Hz, which is the lowest frequency.

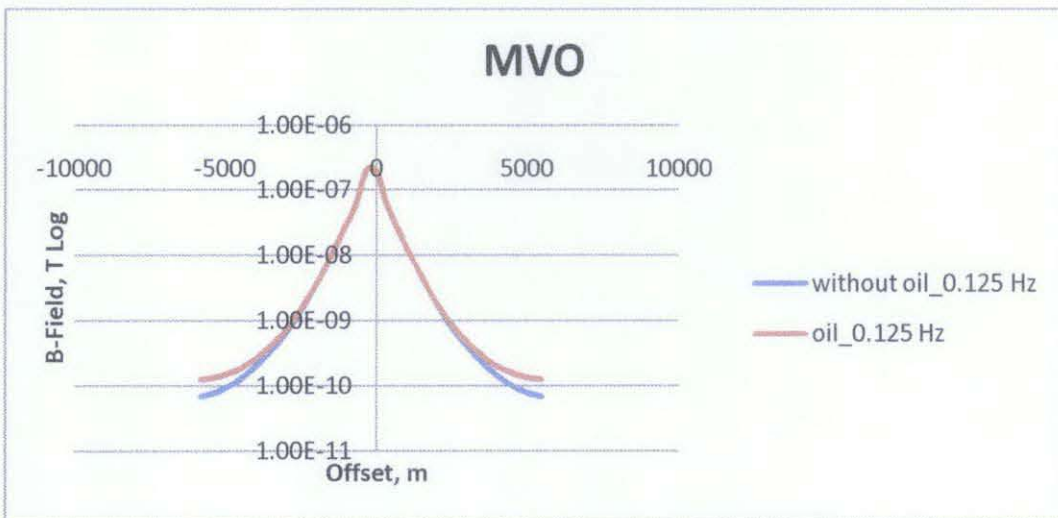


Figure 20: Magnitude versus Offset, 0.125 Hz

From Figure 20, red line denoted the seabed that contains hydrocarbon and blue line denoted the seabed without hydrocarbon. In Figure 21 (0.25 Hz), 22 (0.5 Hz), and 23 (1 Hz), it gives the same result as in Figure 20. But, the different is the low frequency gives higher magnitude of B-Field. This is due to the attenuation of the EM waves, which is higher for high frequency. Figure 24 show the behavior of attenuation of EM wave with different frequency.

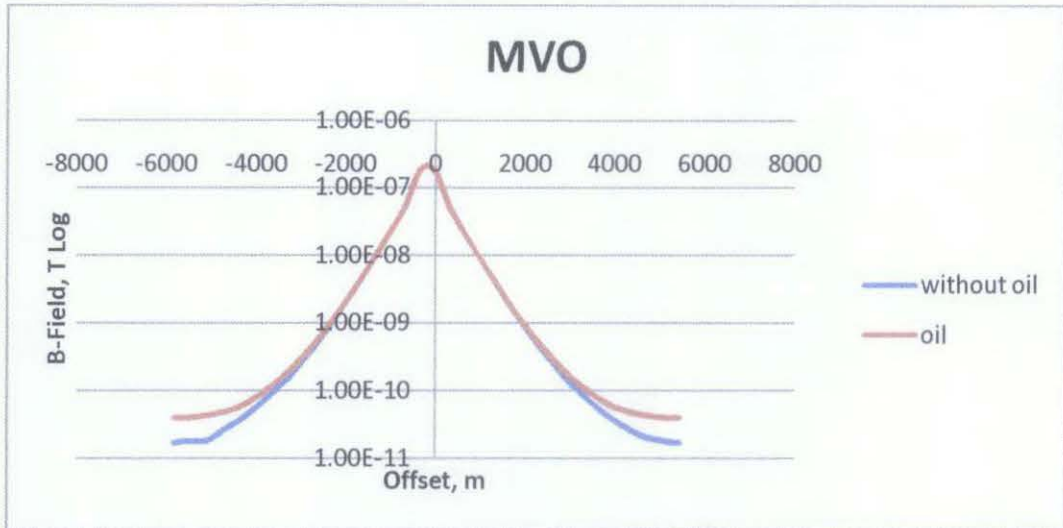


Figure 21: Magnitude versus Offset, 0.25 Hz

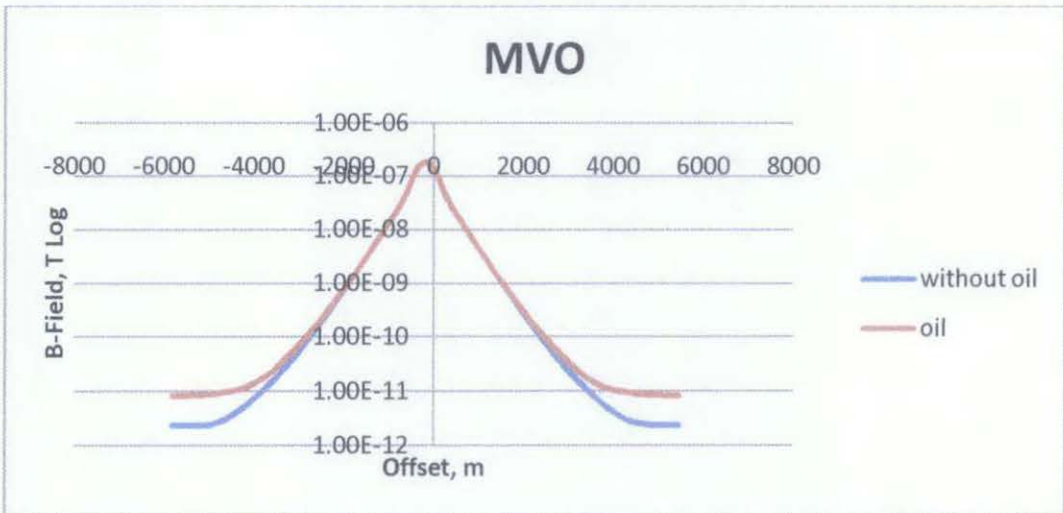


Figure 22: Magnitude versus Offset, 0.5 Hz

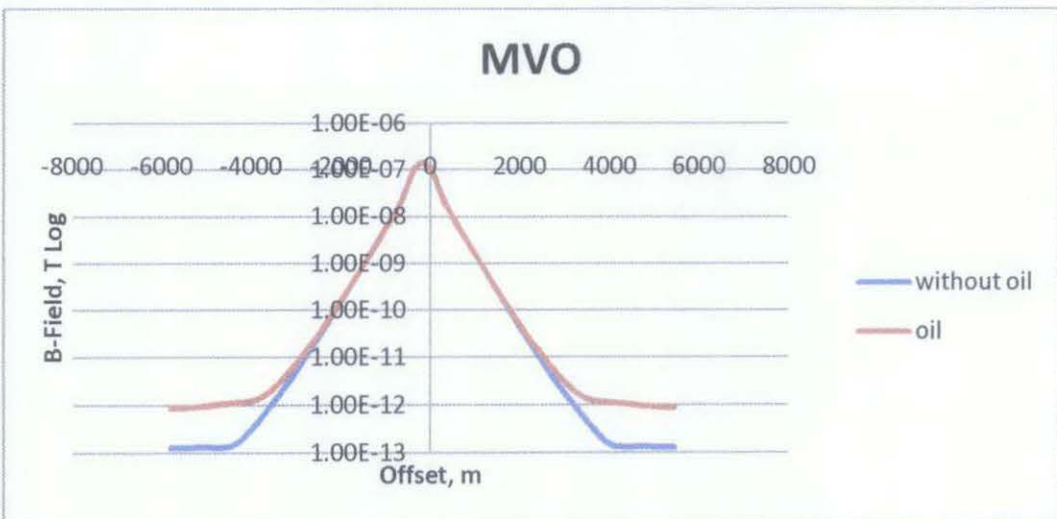


Figure 23: Magnitude versus Offset, 1 Hz

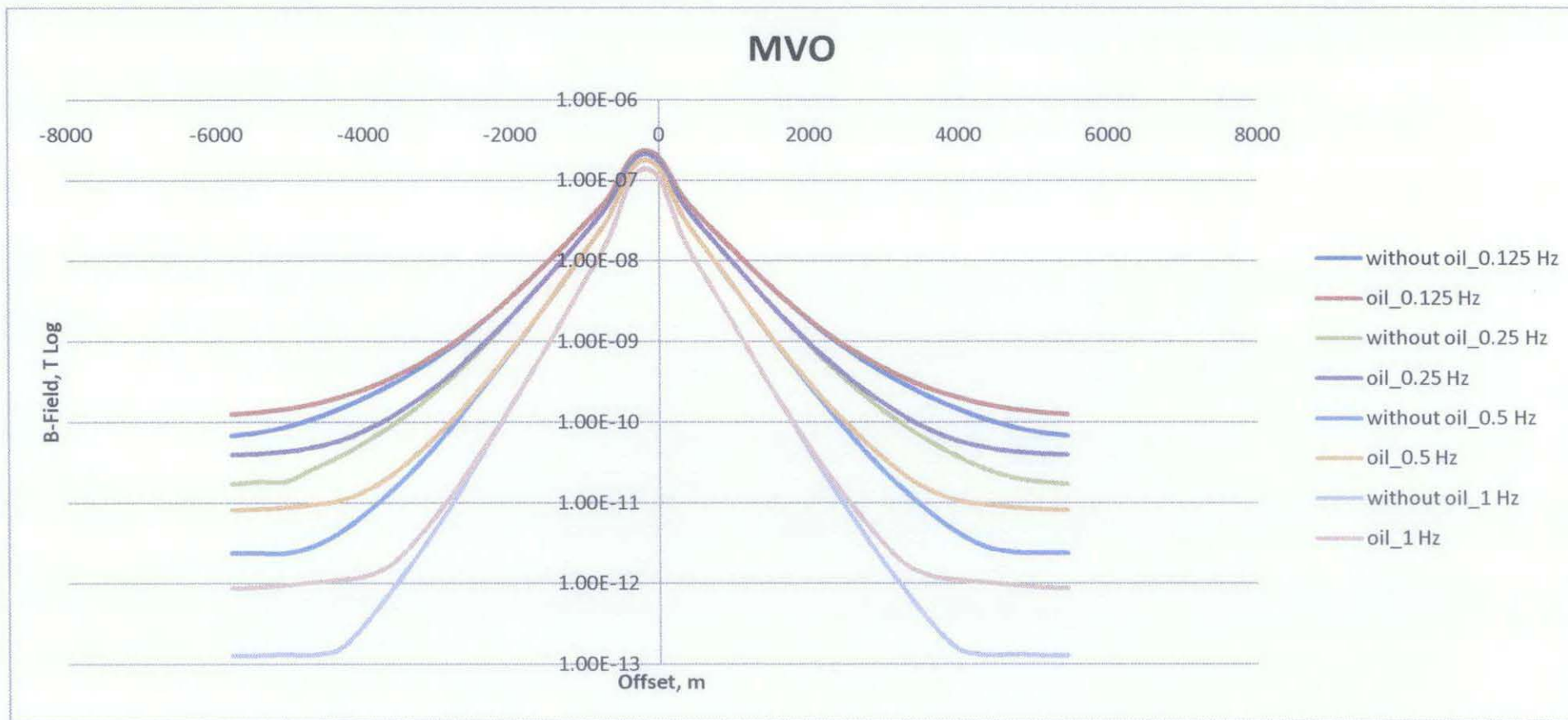


Figure 24: Magnitude versus Offset, 0.125 Hz, 0.25 Hz, 0.5 Hz, 1 Hz

Table 2 shows the percentage difference for seafloor with hydrocarbon and without hydrocarbon in full scale simulation.

Table 2: Percentage, % Difference for Seafloor with Hydrocarbon and Without Hydrocarbon (Full Scale)

Magnitude of B-Field at Offset 6000 m			
Frequency, Hz	Without Hydrocarbon	With Hydrocarbon	% Difference
0.125	6.80E-11	1.26E-10	85.74
0.25	1.73E-11	3.97E-11	129.15
0.5	2.38E-12	8.24E-12	245.41
1	1.28E-13	8.78E-13	583.84

From Table 2, low frequency, 0.125 Hz has lower percentage, 85.74 % compared to high frequency, 1 Hz that gives 583.84 %. This result has shown that the resolution of data is higher for lower frequency at depth of 1000 m of overburden.

4.4 Simulation 4 – Effect of Different Depth of Overburden (Full Scale)

In simulation 4, the depth of the overburden will be varied from 400 m up until the receiver can no longer detect the reflected EM energy from the seabed. Figure 25 shows the result by transmitting 0.125 Hz of EM wave.

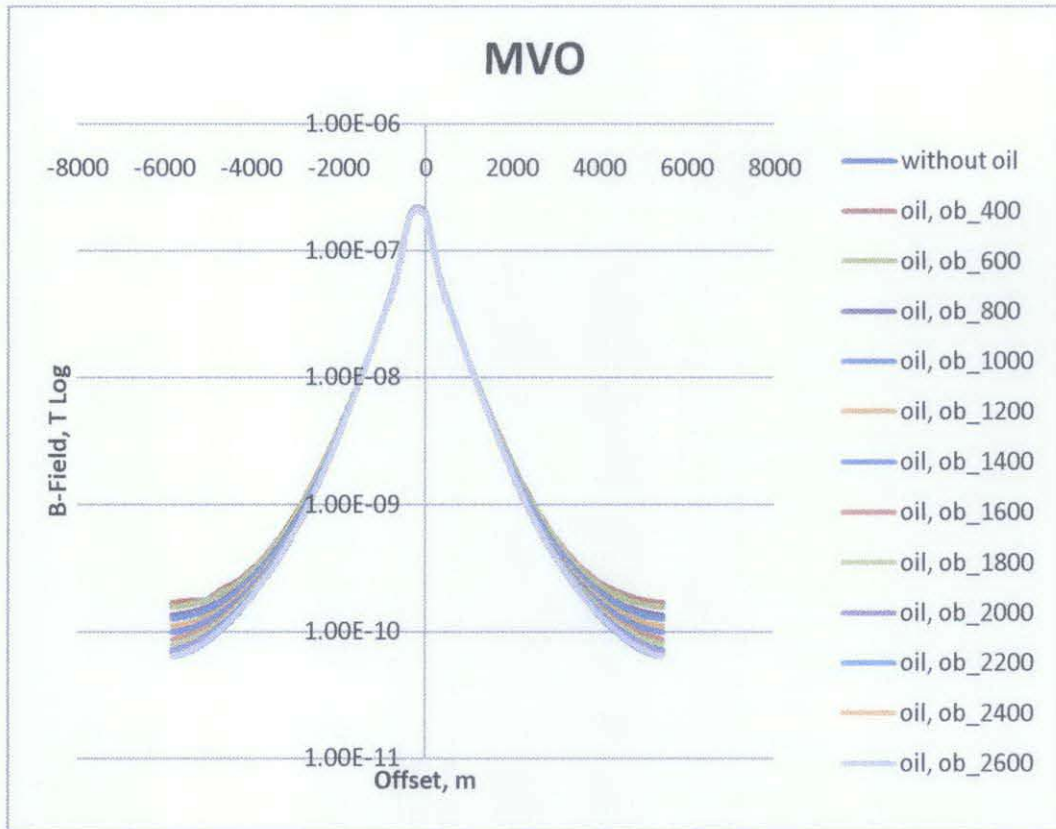


Figure 25: Magnitude versus Offset, Different Depth of Overburden at 0.125 Hz

From Figure 25, at the depth of 2600m, the receiver received repeated data of EM energy reflected from the seabed. This result shows us that the penetration of EM energy has limitation, which is up until this point. Same result is shown in Figure 26 (0.25 Hz), Figure 27 (0.5 Hz), and Figure 28 (1 Hz). If we compare these four results, there is a different at the magnitude of B-Field at each depth of overburden. For example, at the depth of 400m, the magnitude of B-Field is higher for 0.125 Hz of EM wave's frequency. These results again prove that low frequency will gives higher magnitude of B-Field.

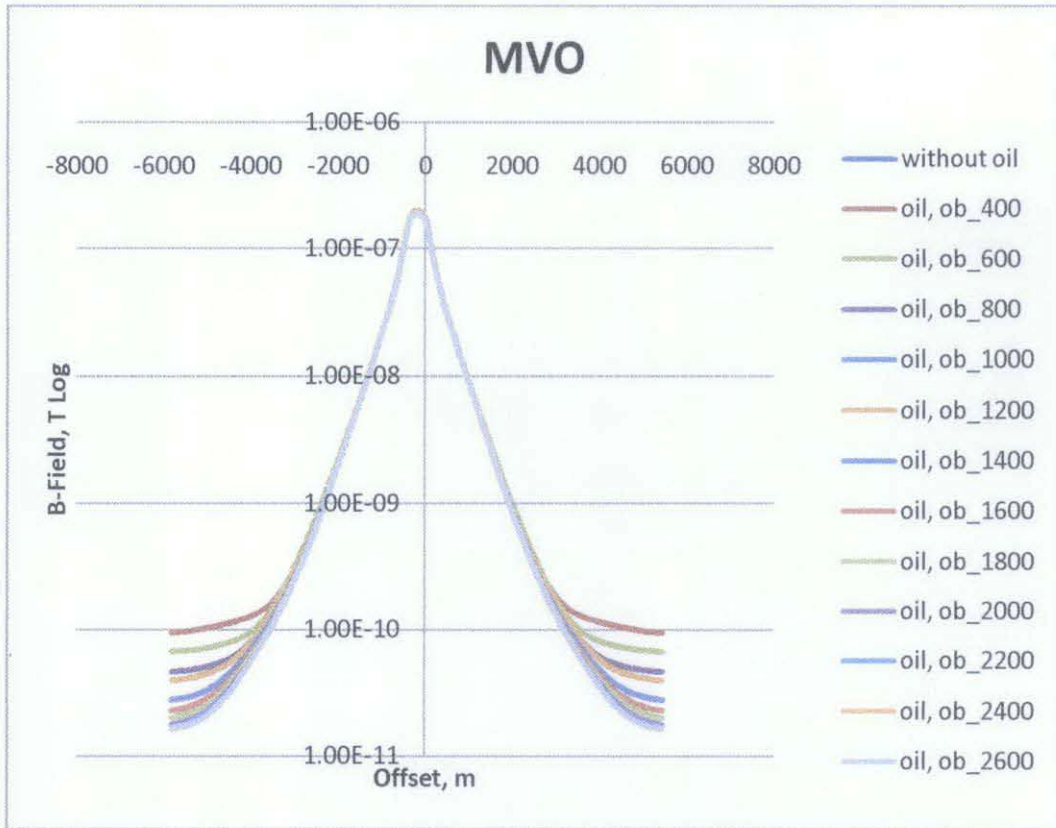


Figure 26: Magnitude versus Offset, Different Depth of Overburden at 0.25 Hz

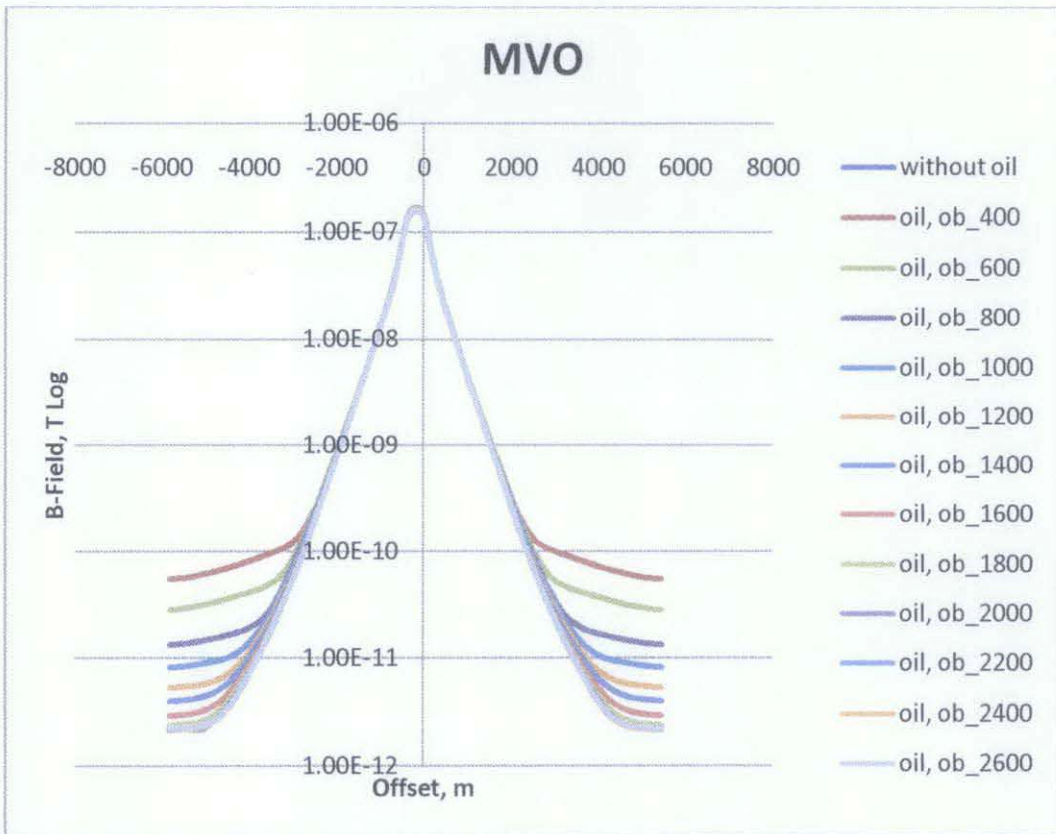


Figure 27: Magnitude versus Offset, Different Depth of Overburden at 0.5 Hz

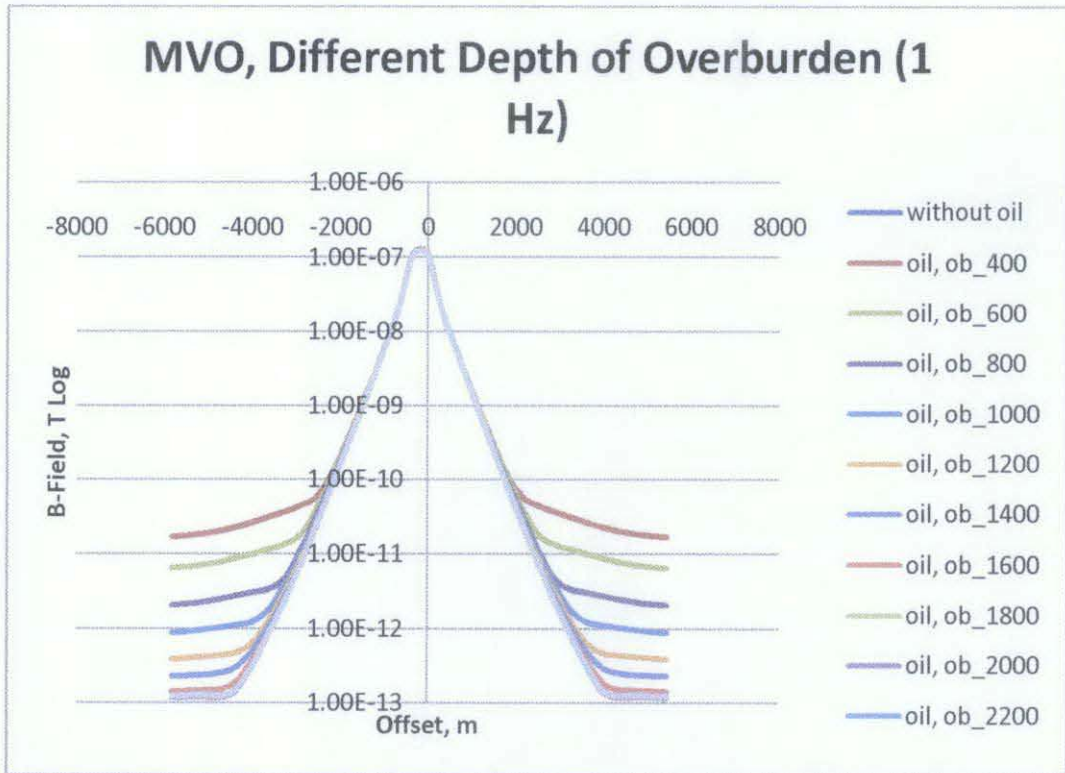


Figure 28: Magnitude versus Offset, Different Depth of Overburden at 1 Hz

Table 3 shows the percentage difference for different depth of overburden for full scale simulation. The result shows for two frequencies which is 0.125 Hz and 0.5 Hz. We can observe that the percentage difference is decrease for both frequencies as the depth of overburden increase. This is due to attenuation of EM waves. From the result also, we can observe that for low frequency, 0.125 Hz, the percentage difference is lower compare to high frequency, 0.5 Hz for depth of 400 m – 1400 m. But the percentage difference for 0.125 Hz becomes higher for depth of 1600 m – 2600 m. This result has shown that low frequency have low resolution of data but less attenuated. Thus, low frequency is best used for deep target exploration.

Table 3: Percentage, % Difference for Different Depth of Overburden
(Full Scale)

Magnitude of B-Field at Offset 6000 m						
Depth, m	Without Hydrocarbon, 0.125 Hz	With Hydrocarbon, 0.125 Hz	% Difference	Without Hydrocarbon, 0.5 Hz	With Hydrocarbon, 0.5 Hz	% Difference
400	6.30E-11	1.69E-10	168.55	2.28E-12	2.28E-12	0
600	6.30E-11	1.56E-10	147.95	2.28E-12	2.84E-11	1,148.24
800	6.30E-11	1.34E-10	113.21	2.28E-12	1.33E-11	481.91
1000	6.30E-11	1.26E-10	100.38	2.28E-12	8.24E-12	261.48
1200	6.30E-11	1.10E-10	74.75	2.28E-12	5.36E-12	135.39
1400	6.30E-11	9.88E-11	56.76	2.28E-12	4.03E-12	76.79
1600	6.30E-11	8.65E-11	37.29	2.28E-12	2.97E-12	30.29
1800	6.30E-11	7.95E-11	26.19	2.28E-12	2.44E-12	6.85
2000	6.30E-11	7.17E-11	13.72	2.28E-12	2.20E-12	3.33
2200	6.30E-11	6.81E-11	8.00	2.28E-12	2.20E-12	3.39
2400	6.30E-11	6.42E-11	1.92	2.28E-12	2.22E-12	2.76
2600	6.30E-11	6.34E-11	0.60	2.28E-12	2.27E-12	0.27

4.5 Simulation 5 – Effect of Different Frequency (Lab Scale)

For simulation 5 and 6, we want to see the effect of different frequency and medium resistivity on propagation of EM waves in lab scale. For simulation 5, the frequency used is 0.78 MHz, 1.56 MHz, 3.13 MHz, and 6.25 MHz. The value of frequency used is calculated by using equation (8). The depth of overburden used is 40 cm. Figure 29 shows the result for 0.78 MHz of EM wave.

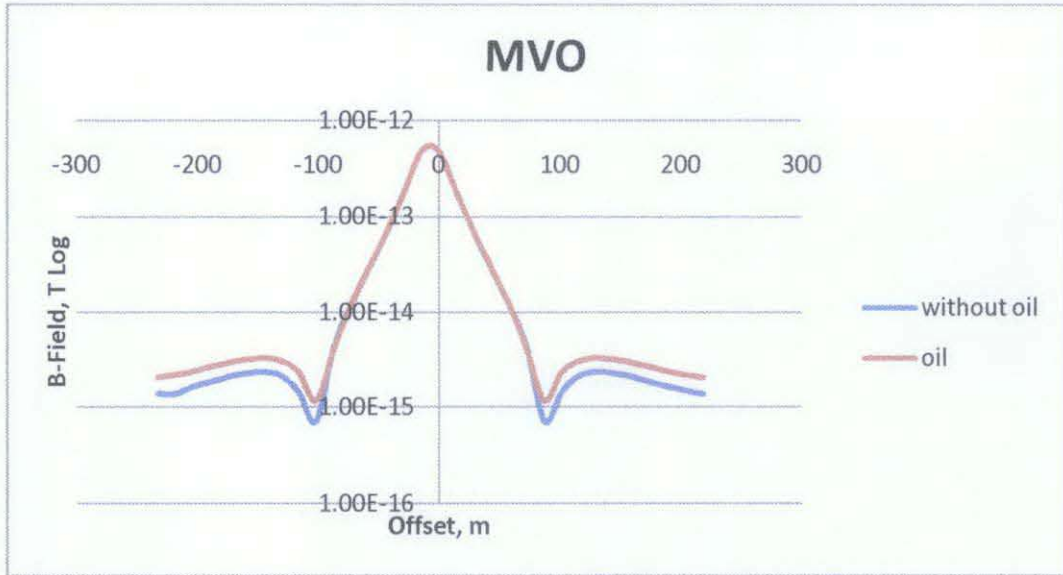


Figure 29: Magnitude versus Offset, 0.78 MHz

From Figure 29, it shows the difference in magnitude of B-Field when the EM wave is penetrated into the seabed that contains the hydrocarbon. In Figure 30(1.56 MHz), Figure 31(3.13 MHz) and Figure 32(6.25 MHz), the result is the same for other frequency except that the one with low frequency gives higher magnitude of B-Field. Figure 33 show the behavior of attenuation of EM wave with different frequency. The result of simulation from lab scale shows the same behavior with the result from full scale.

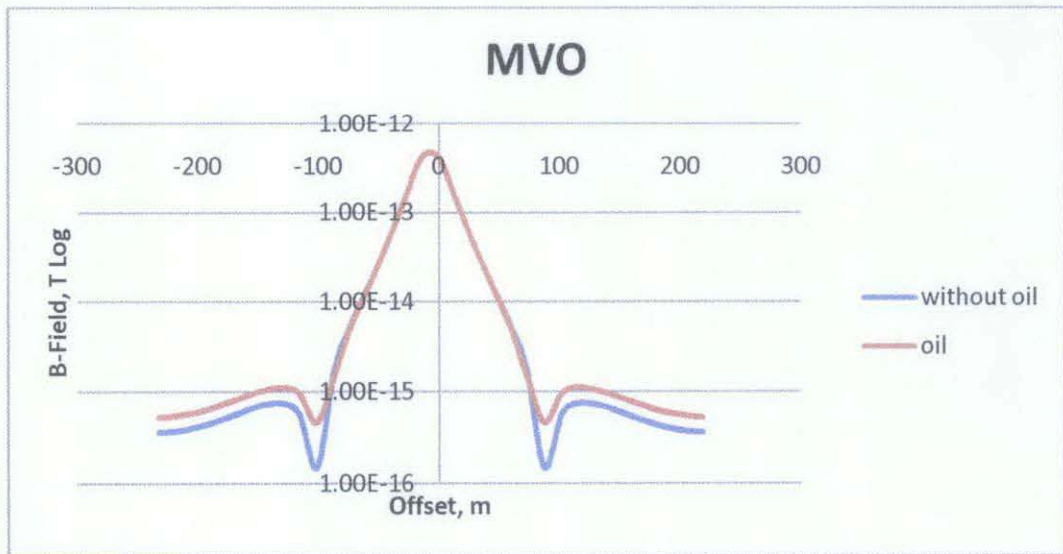


Figure 30: Magnitude versus Offset, 1.56 MHz

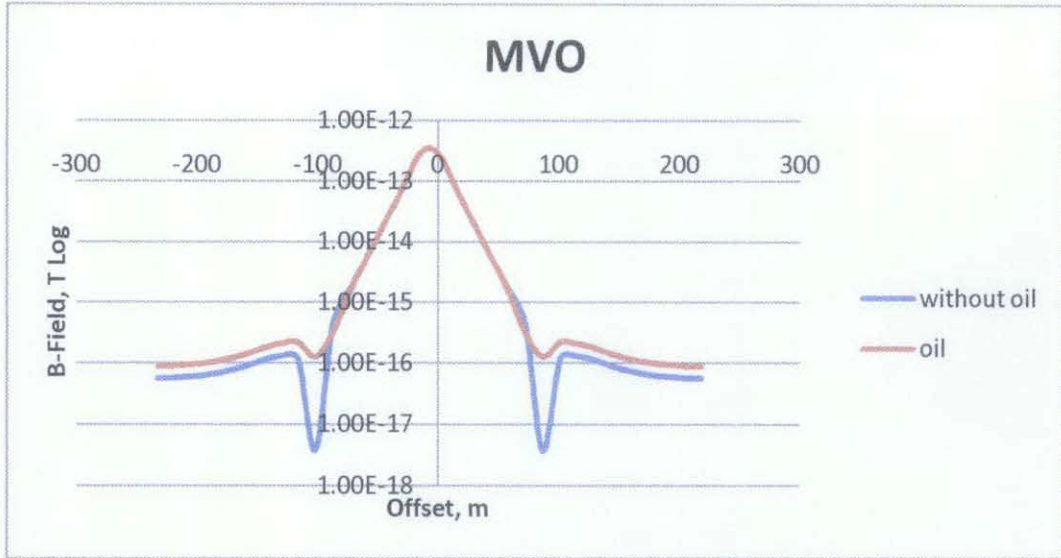


Figure 31: Magnitude versus Offset, 3.13 MHz

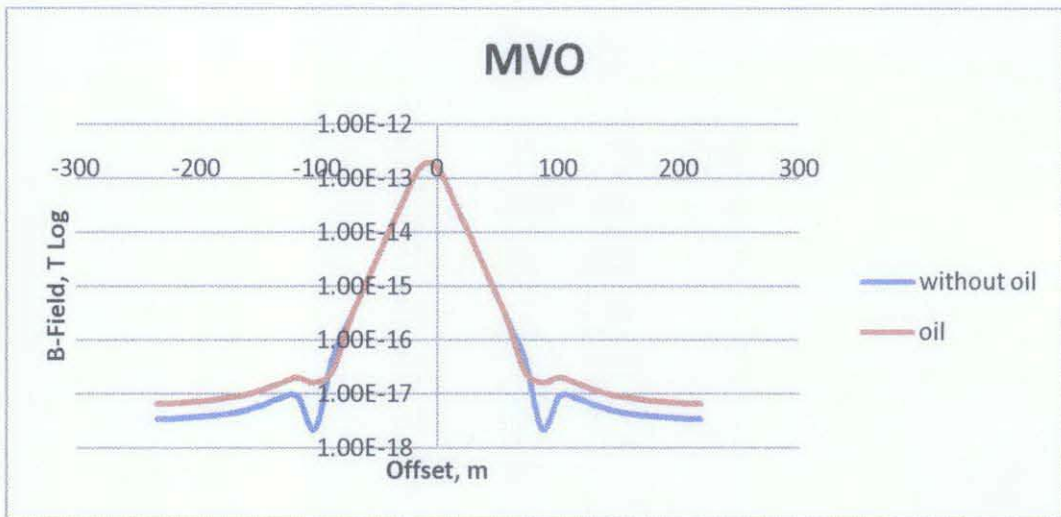


Figure 32: Magnitude versus Offset, 6.25 MHz

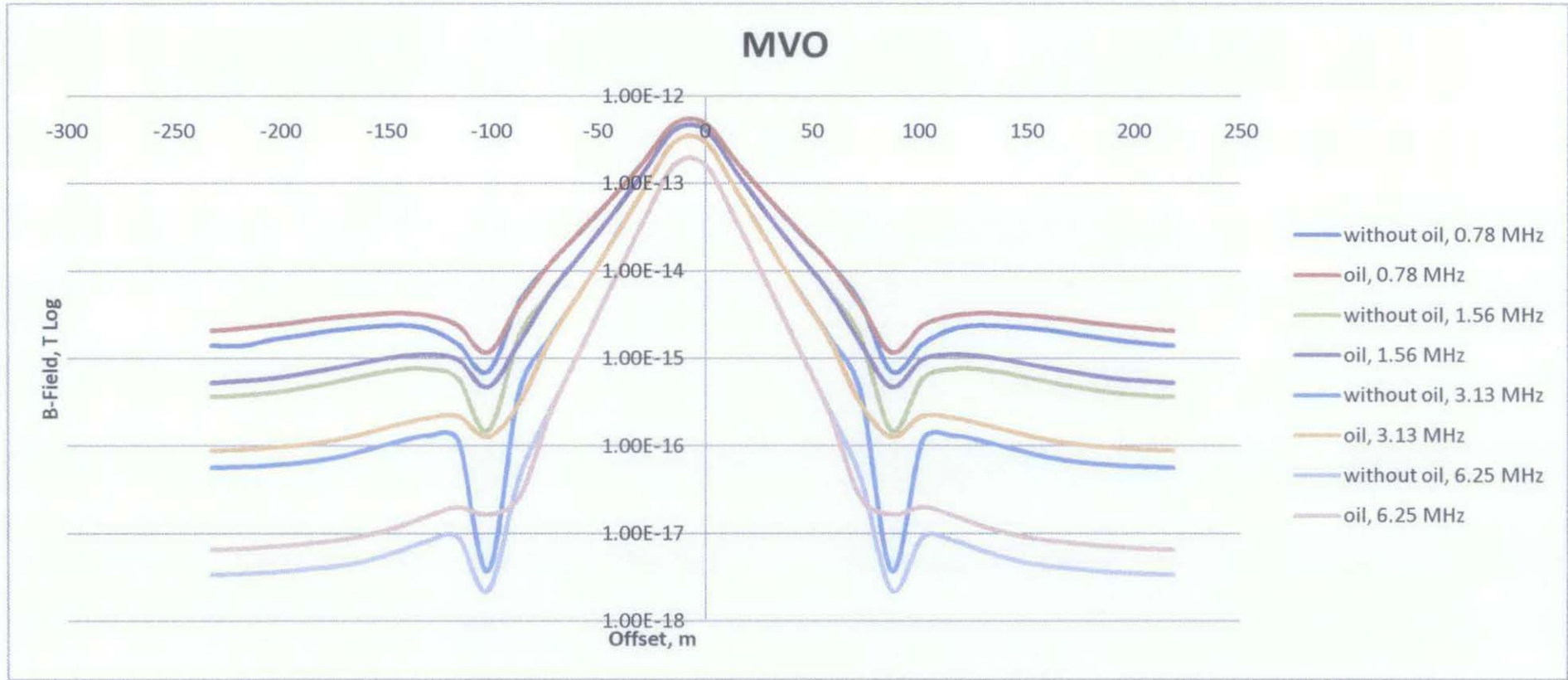


Figure 33: Magnitude versus Offset, 0.78 MHz, 1.56 MHz, 3.13 MHz, 6.25 MHz

Table 4 shows the percentage difference for seafloor with hydrocarbon and without hydrocarbon in lab scale simulation.

Table 4: Percentage, % Difference for Seafloor with Hydrocarbon and Without Hydrocarbon (Lab Scale)

Frequency, Hz	Without Hydrocarbon	With Hydrocarbon	% Difference
0.78	1.39E-15	2.09E-15	49.87
1.56	3.67E-16	5.29E-16	44.35
3.13	5.70E-17	8.94E-17	56.97
6.25	3.39E-18	6.52E-18	92.45

From Table 4, low frequency, 0.78 MHz has lower percentage difference, 49.87 % compared to high frequency, 6.25 MHz that gives 92.45 %. This result has shown the similarity with full scale result for different frequency. The resolution of data at depth of 40 cm is higher for high frequency.

4.6 Simulation 6 – Effect of Different Depth of Overburden (Lab Scale)

For simulation 6, we varied the depth of overburden from 16 cm up until the receiver gives the same magnitude of B-Field. Figure 34 shows the result for 0.78 MHz of EM wave frequency.

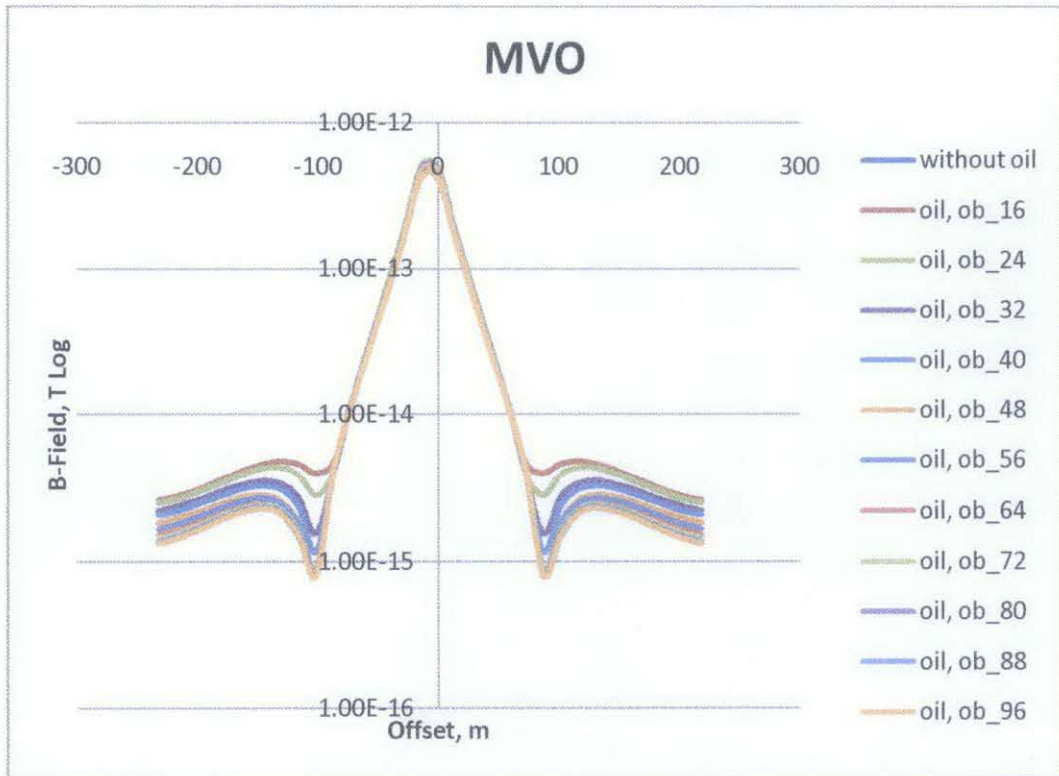


Figure 34: Magnitude versus Offset, Different Depth of Overburden at 0.78 MHz

From Figure 34, the receiver gives repeated data at the depth of 96 cm. Figure 35(1.56 MHz), Figure 36(3.13 MHz), and Figure 37(6.25 MHz) show the same result as in Figure 34. And again, we can see that low frequency gives higher magnitude of B-Field at the receiver.

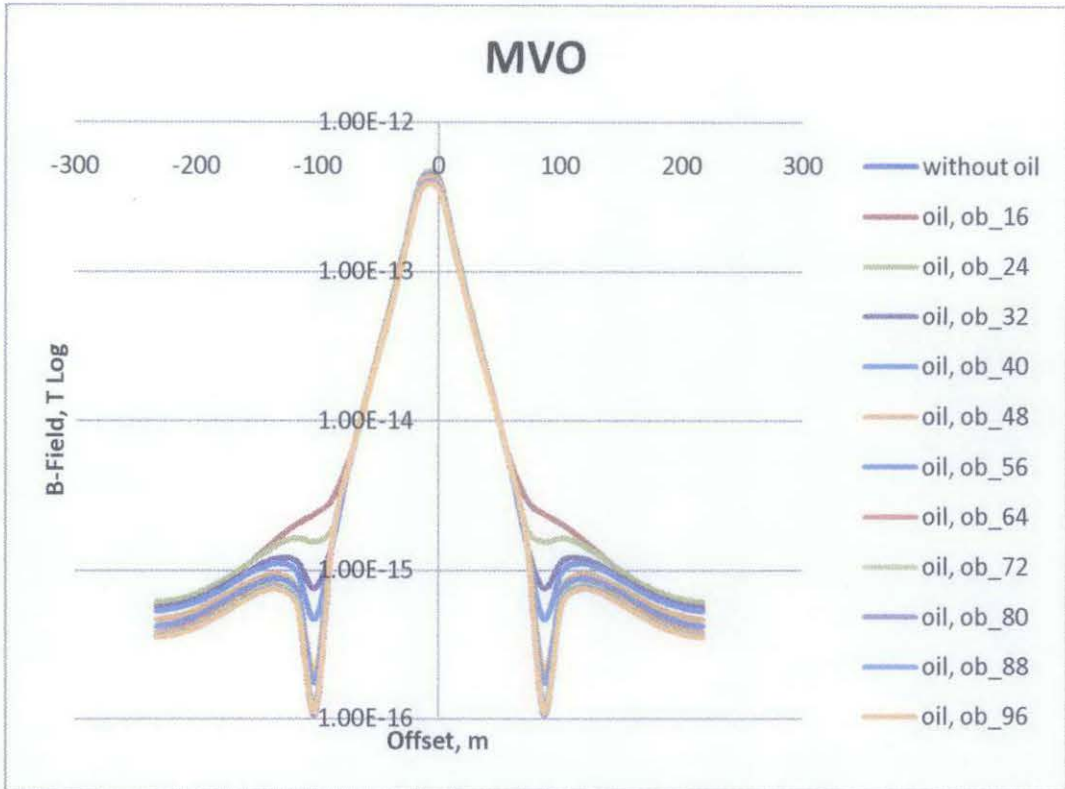


Figure 35: Magnitude versus Offset, Different Depth of Overburden at 1.56 MHz

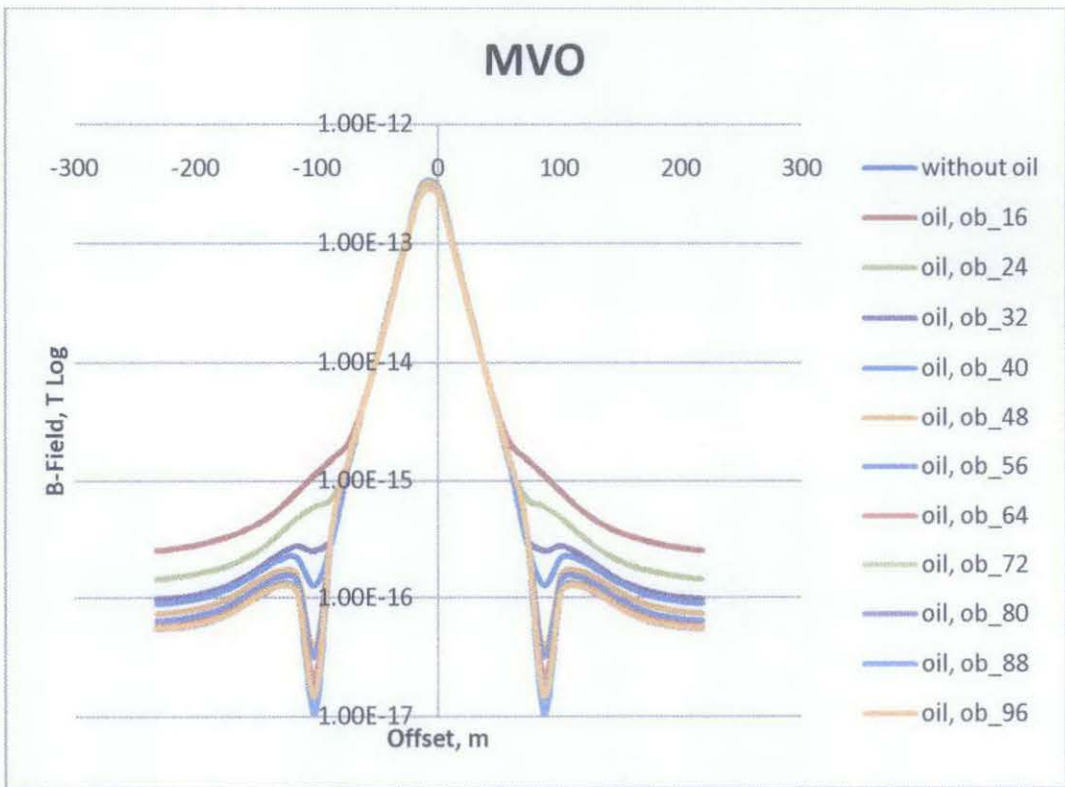


Figure 36: Magnitude versus Offset, Different Depth of Overburden at 3.13 MHz

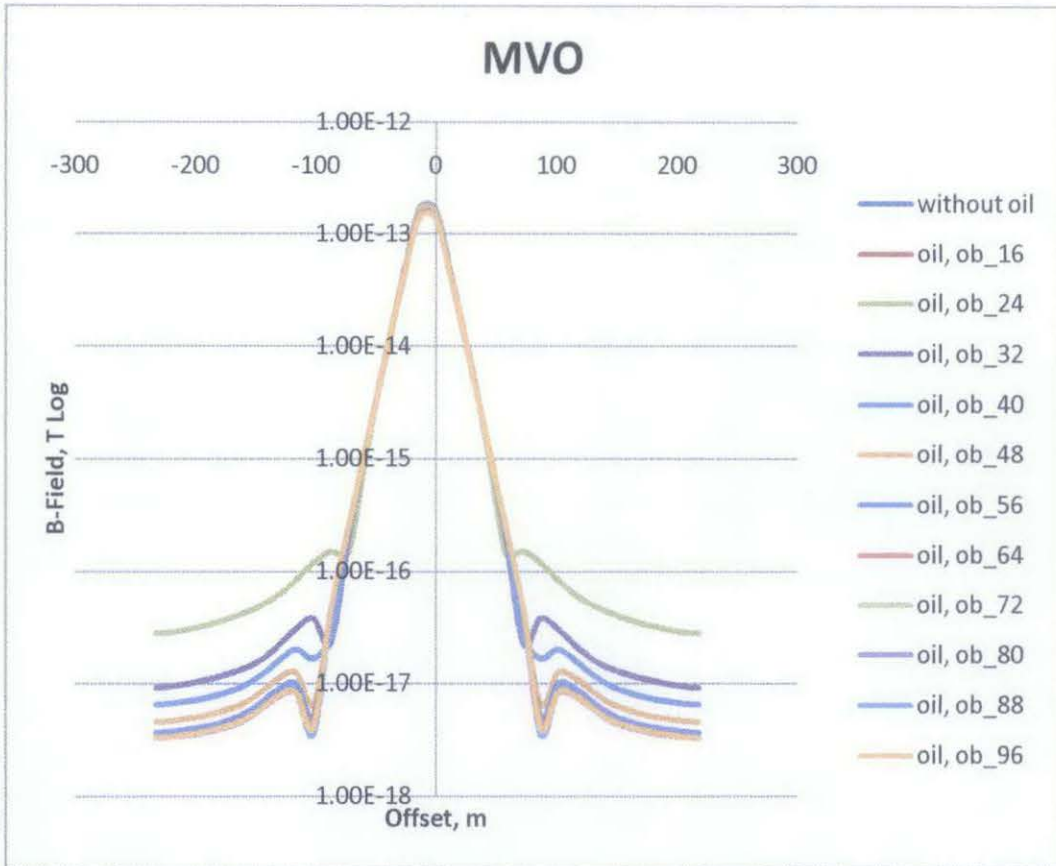


Figure 37: Magnitude versus Offset, Different Depth of Overburden at 6.25MHz

Table 5 shows the percentage difference for different depth of overburden for lab scale simulation. The result shows for two frequencies which is 0.78 MHz and 3.13 MHz. We can observe that the percentage difference is decrease for both frequencies as the depth of overburden increase, due to attenuation of EM waves. From the result also, we can see that for low frequency, 0.78 MHz, the percentage difference is lower compare to high frequency, 3.13 MHz for depth of 16 cm – 40 cm. But the percentage difference for 0.78 MHz becomes higher for depth of 48 cm – 96 cm. This result shows the similarity with the result of full scale. It shows that low frequency have lower resolution of data but less attenuated.

Table 5: Percentage, % Difference for Different Depth of Overburden (Lab Scale)

Magnitude of B-Field at Offset 240 cm						
Depth , cm	Without Hydrocarbon , 0.78 Mhz	With Hydrocarbon , 0.78 Mhz	% Difference	Without Hydrocarbon, 3.13 Mhz	With Hydrocarbon, 3.13 Mhz	% Difference
16	1.35E-15	2.62E-15	94.17	5.58E-17	2.53E-16	354.14
24	1.35E-15	2.52E-15	86.42	5.58E-17	1.44E-16	158.87
32	1.35E-15	2.23E-15	65.28	5.58E-17	9.72E-17	74.21
40	1.35E-15	2.09E-15	54.65	5.58E-17	8.94E-17	60.27
48	1.35E-15	1.84E-15	36.61	5.58E-17	7.36E-17	32.01
56	1.35E-15	1.68E-15	24.29	5.58E-17	6.41E-17	14.85
64	1.35E-15	1.52E-15	12.74	5.58E-17	5.74E-17	2.89
72	1.35E-15	1.45E-15	7.22	5.58E-17	5.57E-17	0.09
80	1.35E-15	1.37E-15	1.75	5.58E-17	5.50E-17	1.48
88	1.35E-15	1.35E-15	0.37	5.58E-17	5.58E-17	0.02
96	1.35E-15	1.33E-15	1.52	5.58E-17	5.56E-17	0.34

4.7 Discussion

4.7.1 Effect of Frequency and Medium Resistivity on Propagation of EM waves

The main focus of this research is to study the effect of different frequency on the propagation of EM wave and how it will affect the reading at the receiver. From simulation results, we can see the differences in the reading of the data when we changed the value of frequency. For simulation 1, we want to see the effect of using lower and higher

frequency when it goes through resistivity medium. In this simulation, we use resistivity medium of sea water and soil. From Figure 17 and 18, the frequency of 0.78 MHz gives highest magnitude of B-Field compare to others. This is due to the attenuation of EM waves. As the magnitude of frequency decreased, the EM waves propagate with higher speed and relatively low attenuation. This result agrees with the theory which is low frequency gives less attenuation of the EM wave. In SBL method, low attenuation of EM wave is needed in order to get higher reading at the receiver.

Next simulation is we want to see the propagation of EM waves in different resistivity medium with constant frequency, 0.78 MHz. From Figure 19, the magnitude of B-Field is higher for soil, followed by sea water and air. This result shows us that when the resistivity of medium is increased, the magnitude of B-Field at the receiver increased due to high reflection of EM waves from the reservoir. From theory, high resistivity will give bigger skin depth. When the skin depth is bigger, the attenuation of EM wave will be less. Thus, the result from this simulation agreed with the theoretical view.

4.7.2 Effect of EM Wave with Different Frequency in SBL

From the result, whether in full scale or lab scale dimensions, there is a difference in magnitude of B-Field when we changed from low frequency to high frequency. For example, we can compare the MVO of Figure 20 and Figure 21. In Figure 20, the magnitude of B-Field shows the difference between the seafloor that have oil and without oil received by the receiver, which is $1.00\text{E}-10$ Tesla. Compare to Figure 21, the reading is lower, which is close to $1.00\text{E}-11$ Tesla. Same thing happen when we increase the frequency, the reading at the receiver become lower. Thus, this simulation agrees with previous simulation, which is lower frequency will give less attenuation of EM waves.

From the result, we can also observe the differences in the data from subsurface that has oil and without oil at 2000 meter offset and above. This happens because at 0 meter offset, the receiver received a direct wave from the transmitter. The direct wave masked the entire signal that has been reflected by the hydrocarbon. The direct wave can only be neglected if the distance between transmitter and receiver is large.

The result from Table 2 and 4 has shown that the percentage difference between seafloor without hydrocarbon and with hydrocarbon. Both tables have shown that high frequency gives better resolution of data for depth of 1000 m in full scale and 40 cm in lab scale.

4.7.3 Effect of EM Wave with Different Depth of Overburden in SBL

In SBL, the thickness of the overburden will also affect the reading of EM wave energy at the receiver. By using the same frequency which is 0.125 Hz – 1 Hz for full scale, and 0.78 MHz – 6.25 MHz for lab scale, we change the thickness of the overburden from 400 m and above until we can obtain the same value or none from the receiver. From Figure 25, we can see the receiver read the energy of EM wave up until 2600 m. If we add the thickness higher than that, the receiver will only show the same value of B-Field. The result also shown that, as the thickness of overburden is decreased, or we can say the closer the hydrocarbon to the source of EM wave, the higher the reading will be.

The result from Table 3 and 5 shows the difference in data resolution. From both tables, it shows that the percentage difference is decreased when the depth of overburden is increased. This is due to the attenuation of EM waves. From the tables also, we can observe that lower frequency has lower percentage difference than high frequency for shallow depth of overburden, and has high percentage difference for deep depth of

overburden. Thus, lower frequency is best used for deep target exploration since it is less attenuated compare to high frequency.

CHAPTER 5

CONCLUSION AND RECOMMENDATION

This chapter explains the conclusions that have been made from the result of the simulations. Several recommendations also included after the study of the project.

5.1 Conclusion

The purpose of this simulation is to study the effect of using different frequency and resistive medium on the propagation of EM wave. The result of the simulation shows that the differences in frequency and thickness of overburden affect the reading of EM energy at the receiver.

MVO is higher for low frequency. This is because EM wave is less attenuated for low frequency due to bigger skin depth. Thus, we can use low frequency in deep target exploration since lower frequency can propagate the EM wave for longer distance with higher value of B-Field compare to higher frequency. It is also shown that different resistive medium also affect the propagation of EM waves. As the conductivity of resistive medium is increased, the EM waves will attenuate more.

From the result of different depth of overburden, it shows that when the depth of the overburden is increase, the MVO decrease. This is due to the attenuation of EM waves as it goes for longer distance in resistive medium.

From the tables, we can observe that high frequency can give high resolution, but less penetration compare to low frequency. Thus, low frequency is best used in deep water exploration.

5.2 Recommendation

The results obtained in this research are relevant with the objectives. If this project is expanded in wider scope like considering more parameters, we will be able to study a lot more theories and in the same time gain more knowledge in applied sciences. It is suggested in this research for several recommendations:

- a) To upgrade the design of the transmitter in order to get higher reading.
- b) To design a seabed structure exactly like the real seabed by considering other parameters such as thermal capacity and density of the sediment and hydrocarbon.
- c) To study on the shallow water exploration.

REFERENCES

- [1] Journal of Applied Geophysics, Volume 64, Pages 47-55

- [2] Ellingsrud et al. The Leading Edge.2002; 21: 972-982

- [3] Baldwin, W.E., Morton, R.A., Denny, J.F., Dadisman, S.V., Schwab, W.C., Gayes, P.T., and Driscoll, N.W., 2004, Maps showing the stratigraphic framework of South Carolina's Long Bay from Little River to Winyah Bay, U.S. Geological Survey Open-File Report 2004-1013.

- [4] Foster, D.S., McKinney, B.A., and Schwab, W.C., 1999, Stratigraphic Framework Maps of the Nearshore Area of Southern Long Island from Fire Island to Montauk Point, New York: U.S. Geological Survey Open File Report 99-559.

- [5] Birch, F.S., 1976, A seismic ground-water survey in New Hampshire, Ground Water, v. 14, n. 2, pp. 94-100

- [6] Sheriff, R. E., and Geldart, L. P., 1995, Exploration Seismology, Second Edition, Cambridge University Press, 3-6

- [7] Eidesmo, T., Ellingsrud, S., MacGregor, L.M., Constable, S., Sinha, M.C., Westerdahl, H., and Kong, F.N., "Remote detection of hydrocarbon filled layers using marine controlled source electromagnetic sounding," paper submitted to EAGE 64th Conference & Exhibition, Florence, Italy, May 27-30, 2002

- [8] Chave, A.D., Constable, S.C., and Edwards, N., "Electrical exploration methods for the seafloor," in Nabighian, M., ed., "Electromagnetic Methods in Applied Geophysics," Vol. 2, SEG, Tulsa, Okla., 1991, pp. 931-966
- [9] "Challenges in Shallow Water CSEM Surveying: A Case History from Southeast Asia", Sandeep K. Chandola*, Rashidah Karim, Amy Mawarni, Russikin Ismail, Noreehan Shahud, Ramlee Rahman, Paul Bernabe ; PETRONAS Carigali Sdn. Bhd., Kuala Lumpur, Malaysia ; Ketil Brauti, EMGS AS, Trondheim (Presented at International Petroleum Technology Conference held in Dubai, U.A.E, 4-8 December 2007)
- [10] Eidesmo, T., Ellingsrud, S., MacGregor, L.M., Constable, S., Sinha, M.C., Johansen, S., and Kong, F.N., "Seabed logging (SBL), a new method for remote and direct identification of hydrocarbon-filled layers in deepwater areas," *First Break*, Vol. 20, 2002, pp.144–152
- [11] Anonymous, "An exploration renaissance," *Changes*, Vol. 6 (1), 2005, pp. 4–7
- [12] Johansen, S., Amundsen, H.E.F., Røsten, T., Ellingsrud, S., Eidesmo, T., and Bhuyian, A.H., "Subsurface hydrocarbons detected by electromagnetic sounding," *First Break*, Vol. 23, 2005, pp. 31–36.
- [13] <http://www.emgs.com/content/583/EMGS-extends-CSEM-water-depth-record>
- [14] Shallow water 3D CSEM: A case study from Malaysia :Håkon Toralv Pedersen*, EMGS ASA, M. Akmal Affendi B. Adnan, Azani B. A. Manaf, Petronas
- [15] James Clerk Maxwell, "A Dynamical Theory of the Electromagnetic Field", *Philosophical Transactions of the Royal Society of London* 155, 459-512

- [16] [http://en.wikipedia.org/wiki/Permeability_\(electromagnetism\)](http://en.wikipedia.org/wiki/Permeability_(electromagnetism))
- [17] <http://en.wikipedia.org/wiki/Permittivity>
- [18] L.-J. Gelius, "Multi-component Processing of Sea Bed Logging Data",
Department of Geoscience, University of Oslo, Norway, PIERS
ONLINE, Vol. 2, No 6 , 2006
- [19] T. E. Faber: Fluid Dynamics for Physicists

APPENDICES

APPENDIX A

Table 6: Gantt Chart for FYP I

No	Detail / Week	1	2	3	4	5	6	7	8	9	10	11	12	13	14
1	Topic Selection														
2	Research on SeaBed Logging & EM Wave														
3	Submission of Preliminary Report														
4	Simulation Work														
5	Submission Progress Report														
6	Seminar														
7	Continue project work														
8	Submission of Interim Report Final Draft														
9	Oral Presentation														
10	Submission of Final Report														

APPENDIX B

Table 7: Gant Chart for FYP II

No	Detail / Week	1	2	3	4	5	6	7	8	9	10	11	12	13	14
1	Project Work Continue														
2	Submission of Progress Report 1														
3	Project Work Continue														
4	Submission of Progress Report 2														
5	Project Work Continue														
6	Submission of Draft Report														
7	Submission of Final Report														
8	Submission of Technical Report														
9	Oral Presentation														
10	Final Report														

APPENDIX C

Raw Reading for Simulation 1

Length		Offset, seawater	0.78 MHz	1.56 MHz	3.13 MHz	6.25 MHz		Offset, air	0.78 MHz	1.56 MHz	3.13 MHz	6.25 MHz
7.28125		-232.71875	1.40E-17	7.90E-19	1.00E-20	1.47E-23		-232.7188	9.78E-19	5.18E-19	2.78E-19	1.69E-19
21.84375		-218.15625	2.00E-17	1.47E-18	2.76E-20	6.10E-23		-218.1563	9.68E-19	5.17E-19	2.85E-19	1.85E-19
36.40625		-203.59375	3.46E-17	3.25E-18	7.90E-20	2.48E-22		-203.5938	9.50E-19	5.18E-19	3.03E-19	2.17E-19
50.96875		-189.03125	6.31E-17	7.12E-18	2.23E-19	1.01E-21		-189.0313	9.26E-19	5.27E-19	3.42E-19	2.76E-19
65.53125		-174.46875	1.16E-16	1.56E-17	6.30E-19	4.18E-21		-174.4688	8.99E-19	5.61E-19	4.22E-19	3.79E-19
80.09375		-159.90625	2.13E-16	3.42E-17	1.79E-18	1.77E-20		-159.9063	8.87E-19	6.51E-19	5.70E-19	5.47E-19
94.65625		-145.34375	3.95E-16	7.58E-17	5.09E-18	7.68E-20		-145.3438	9.41E-19	8.50E-19	8.23E-19	8.16E-19
109.2187		-130.7813	7.43E-16	1.69E-16	1.47E-17	3.45E-19		-130.7813	1.17E-18	1.23E-18	1.25E-18	1.25E-18
123.7812		-116.2188	1.42E-15	3.83E-16	4.31E-17	1.60E-18		-116.2188	1.74E-18	1.90E-18	1.94E-18	1.95E-18
138.3437		-101.6563	2.76E-15	8.81E-16	1.30E-16	7.65E-18		-101.6563	2.84E-18	3.05E-18	3.11E-18	3.12E-18
152.9062		-87.0938	5.52E-15	2.08E-15	4.11E-16	3.75E-17		-87.0938	4.87E-18	5.06E-18	5.12E-18	5.13E-18
167.4687		-72.5313	1.15E-14	5.15E-15	1.37E-15	1.89E-16		-72.5313	8.64E-18	8.74E-18	8.78E-18	8.79E-18
182.0312		-57.9688	2.53E-14	1.36E-14	4.85E-15	1.00E-15		-57.9688	1.62E-17	1.60E-17	1.60E-17	1.60E-17
196.5937		-43.4063	6.14E-14	3.94E-14	1.86E-14	5.59E-15		-43.4063	3.30E-17	3.22E-17	3.20E-17	3.19E-17
211.1562		-28.8438	1.68E-13	1.27E-13	7.60E-14	3.17E-14		-28.8438	7.64E-17	7.41E-17	7.35E-17	7.33E-17
225.5781		-14.4219	4.76E-13	4.02E-13	2.84E-13	1.49E-13		-14.4219	1.86E-16	1.84E-16	1.84E-16	1.83E-16
239.8594		-0.1406	4.76E-13	4.02E-13	2.84E-13	1.49E-13		-0.1406	1.86E-16	1.84E-16	1.84E-16	1.83E-16
254.2813		14.2813	1.68E-13	1.27E-13	7.60E-14	3.17E-14		14.2813	7.64E-17	7.41E-17	7.35E-17	7.33E-17
268.8438		28.8438	6.14E-14	3.94E-14	1.86E-14	5.59E-15		28.8438	3.30E-17	3.22E-17	3.20E-17	3.19E-17
283.4063		43.4063	2.53E-14	1.36E-14	4.85E-15	1.00E-15		43.4063	1.62E-17	1.60E-17	1.60E-17	1.60E-17
297.9688		57.9688	1.15E-14	5.15E-15	1.37E-15	1.89E-16		57.9688	8.64E-18	8.74E-18	8.78E-18	8.79E-18
312.5313		72.5313	5.52E-15	2.08E-15	4.11E-16	3.75E-17		72.5313	4.87E-18	5.06E-18	5.12E-18	5.13E-18
327.0938		87.0938	2.76E-15	8.81E-16	1.30E-16	7.65E-18		87.0938	2.84E-18	3.05E-18	3.11E-18	3.12E-18
341.6563		101.6563	1.42E-15	3.83E-16	4.31E-17	1.60E-18		101.6563	1.74E-18	1.90E-18	1.94E-18	1.95E-18
356.2188		116.2188	7.43E-16	1.69E-16	1.47E-17	3.45E-19		116.2188	1.17E-18	1.23E-18	1.25E-18	1.25E-18
370.7813		130.7813	3.95E-16	7.58E-17	5.09E-18	7.68E-20		130.7813	9.41E-19	8.50E-19	8.23E-19	8.16E-19
385.3438		145.3438	2.13E-16	3.42E-17	1.79E-18	1.77E-20		145.3438	8.87E-19	6.51E-19	5.70E-19	5.47E-19
399.9063		159.9063	1.16E-16	1.56E-17	6.30E-19	4.18E-21		159.9063	8.99E-19	5.61E-19	4.22E-19	3.79E-19
414.4688		174.4688	6.31E-17	7.12E-18	2.23E-19	1.01E-21		174.4688	9.26E-19	5.27E-19	3.42E-19	2.76E-19
429.0313		189.0313	3.46E-17	3.25E-18	7.90E-20	2.48E-22		189.0313	9.50E-19	5.18E-19	3.03E-19	2.17E-19
443.5938		203.5938	2.00E-17	1.47E-18	2.76E-20	6.10E-23		203.5938	9.68E-19	5.17E-19	2.85E-19	1.85E-19
458.1563		218.1563	1.40E-17	7.90E-19	1.00E-20	1.47E-23		218.1563	9.78E-19	5.18E-19	2.78E-19	1.69E-19

	Offset, soil	0.78 MHz	1.56 MHz	3.13 MHz	6.25 MHz
	-232.71875	4.09E-17	7.00E-18	3.89E-19	5.08E-21
	-218.15625	5.22E-17	1.00E-17	7.27E-19	1.40E-20
	-203.59375	7.66E-17	1.73E-17	1.60E-18	4.00E-20
	-189.03125	1.21E-16	3.16E-17	3.52E-18	1.13E-19
	-174.46875	1.97E-16	5.79E-17	7.70E-18	3.18E-19
	-159.90625	3.24E-16	1.07E-16	1.69E-17	9.02E-19
	-145.34375	5.38E-16	1.98E-16	3.76E-17	2.57E-18
	-130.7813	9.07E-16	3.72E-16	8.40E-17	7.39E-18
	-116.2188	1.55E-15	7.11E-16	1.90E-16	2.17E-17
	-101.6563	2.71E-15	1.38E-15	4.38E-16	6.56E-17
	-87.0938	4.87E-15	2.77E-15	1.04E-15	2.07E-16
	-72.5313	9.11E-15	5.75E-15	2.56E-15	6.87E-16
	-57.9688	1.81E-14	1.27E-14	6.78E-15	2.43E-15
	-43.4063	3.94E-14	3.07E-14	1.97E-14	9.33E-15
	-28.8438	9.78E-14	8.40E-14	6.34E-14	3.81E-14
	-14.4219	2.59E-13	2.38E-13	2.01E-13	1.42E-13
	-0.1406	2.59E-13	2.38E-13	2.01E-13	1.42E-13
	14.2813	9.78E-14	8.40E-14	6.34E-14	3.81E-14
	28.8438	3.94E-14	3.07E-14	1.97E-14	9.33E-15
	43.4063	1.81E-14	1.27E-14	6.78E-15	2.43E-15
	57.9688	9.11E-15	5.75E-15	2.56E-15	6.87E-16
	72.5313	4.87E-15	2.77E-15	1.04E-15	2.07E-16
	87.0938	2.71E-15	1.38E-15	4.38E-16	6.56E-17
	101.6563	1.55E-15	7.11E-16	1.90E-16	2.17E-17
	116.2188	9.07E-16	3.72E-16	8.40E-17	7.39E-18
	130.7813	5.38E-16	1.98E-16	3.76E-17	2.57E-18
	145.3438	3.24E-16	1.07E-16	1.69E-17	9.02E-19
	159.9063	1.97E-16	5.79E-17	7.70E-18	3.18E-19
	174.4688	1.21E-16	3.16E-17	3.52E-18	1.13E-19
	189.0313	7.66E-17	1.73E-17	1.60E-18	4.00E-20
	203.5938	5.22E-17	1.00E-17	7.27E-19	1.40E-20
	218.1563	4.09E-17	7.00E-18	3.89E-19	5.08E-21

APPENDIX D
Raw Reading for Simulation 2

Length		Offset, 0.78 MHz	Seawater	Soil	Air
7.28125		-232.71875	1.40E-17	4.09E-17	9.78E-19
21.84375		-218.15625	2.00E-17	5.22E-17	9.68E-19
36.40625		-203.59375	3.46E-17	7.66E-17	9.50E-19
50.96875		-189.03125	6.31E-17	1.21E-16	9.26E-19
65.53125		-174.46875	1.16E-16	1.97E-16	8.99E-19
80.09375		-159.90625	2.13E-16	3.24E-16	8.87E-19
94.65625		-145.34375	3.95E-16	5.38E-16	9.41E-19
109.2187		-130.7813	7.43E-16	9.07E-16	1.17E-18
123.7812		-116.2188	1.42E-15	1.55E-15	1.74E-18
138.3437		-101.6563	2.76E-15	2.71E-15	2.84E-18
152.9062		-87.0938	5.52E-15	4.87E-15	4.87E-18
167.4687		-72.5313	1.15E-14	9.11E-15	8.64E-18
182.0312		-57.9688	2.53E-14	1.81E-14	1.62E-17
196.5937		-43.4063	6.14E-14	3.94E-14	3.30E-17
211.1562		-28.8438	1.68E-13	9.78E-14	7.64E-17
225.5781		-14.4219	4.76E-13	2.59E-13	1.86E-16
239.8594		-0.1406	4.76E-13	2.59E-13	1.86E-16
254.2813		14.2813	1.68E-13	9.78E-14	7.64E-17
268.8438		28.8438	6.14E-14	3.94E-14	3.30E-17
283.4063		43.4063	2.53E-14	1.81E-14	1.62E-17
297.9688		57.9688	1.15E-14	9.11E-15	8.64E-18
312.5313		72.5313	5.52E-15	4.87E-15	4.87E-18
327.0938		87.0938	2.76E-15	2.71E-15	2.84E-18
341.6563		101.6563	1.42E-15	1.55E-15	1.74E-18
356.2188		116.2188	7.43E-16	9.07E-16	1.17E-18
370.7813		130.7813	3.95E-16	5.38E-16	9.41E-19
385.3438		145.3438	2.13E-16	3.24E-16	8.87E-19
399.9063		159.9063	1.16E-16	1.97E-16	8.99E-19
414.4688		174.4688	6.31E-17	1.21E-16	9.26E-19
429.0313		189.0313	3.46E-17	7.66E-17	9.50E-19
443.5938		203.5938	2.00E-17	5.22E-17	9.68E-19
458.1563		218.1563	1.40E-17	4.09E-17	9.78E-19

APPENDIX E

Raw Reading for Simulation 3

Length	Offset	without oil_0.125 Hz	oil_0.125 Hz	without oil_0.25 Hz	oil_0.25 Hz	without oil_0.5 Hz	oil_0.5 Hz
183.2813	-5816.72	6.80E-11	1.26E-10	1.73E-11	3.97E-11	2.38E-12	8.24E-12
549.8438	-5450.16	7.47E-11	1.33E-10	1.83E-11	4.10E-11	2.40E-12	8.48E-12
916.4063	-5083.59	8.77E-11	1.45E-10	1.83E-11	4.35E-11	2.40E-12	8.88E-12
1282.969	-4717.03	1.10E-10	1.67E-10	2.63E-11	4.87E-11	2.89E-12	9.53E-12
1649.531	-4350.47	1.46E-10	2.03E-10	3.73E-11	5.90E-11	4.25E-12	1.08E-11
2016.094	-3983.91	2.03E-10	2.62E-10	5.71E-11	7.96E-11	7.51E-12	1.40E-11
2382.656	-3617.34	2.98E-10	3.60E-10	9.31E-11	1.20E-10	1.46E-11	2.25E-11
2749.219	-3250.78	4.64E-10	5.29E-10	1.63E-10	1.97E-10	3.08E-11	4.25E-11
3115.781	-2884.22	7.73E-10	8.38E-10	3.12E-10	3.54E-10	7.22E-11	8.94E-11
3482.344	-2517.66	1.39E-09	1.44E-09	6.47E-10	6.92E-10	1.85E-10	2.06E-10
3848.906	-2151.09	2.67E-09	2.70E-09	1.43E-09	1.47E-09	4.99E-10	5.20E-10
4215.469	-1784.53	5.46E-09	5.44E-09	3.32E-09	3.34E-09	1.39E-09	1.41E-09
4582.031	-1417.97	1.17E-08	1.16E-08	7.95E-09	7.94E-09	3.95E-09	3.97E-09
4948.594	-1051.41	2.62E-08	2.61E-08	1.97E-08	1.96E-08	1.15E-08	1.16E-08
5315.156	-684.844	6.29E-08	6.27E-08	5.15E-08	5.15E-08	3.54E-08	3.54E-08
5657.578	-342.422	2.02E-07	2.02E-07	1.82E-07	1.82E-07	1.50E-07	1.50E-07
5975.859	-24.141	2.02E-07	2.02E-07	1.82E-07	1.82E-07	1.50E-07	1.50E-07
6318.281	318.281	6.29E-08	6.27E-08	5.15E-08	5.15E-08	3.54E-08	3.54E-08
6684.844	684.844	2.62E-08	2.61E-08	1.97E-08	1.96E-08	1.15E-08	1.16E-08
7051.406	1051.406	1.17E-08	1.16E-08	7.95E-09	7.94E-09	3.95E-09	3.97E-09
7417.969	1417.969	5.46E-09	5.44E-09	3.32E-09	3.34E-09	1.39E-09	1.41E-09
7784.531	1784.531	2.67E-09	2.70E-09	1.43E-09	1.47E-09	4.99E-10	5.20E-10
8151.094	2151.094	1.39E-09	1.44E-09	6.47E-10	6.92E-10	1.85E-10	2.06E-10
8517.656	2517.656	7.73E-10	8.38E-10	3.12E-10	3.54E-10	7.22E-11	8.94E-11
8884.219	2884.219	4.64E-10	5.29E-10	1.63E-10	1.97E-10	3.08E-11	4.25E-11
9250.781	3250.781	2.98E-10	3.60E-10	9.31E-11	1.20E-10	1.46E-11	2.25E-11
9617.344	3617.344	2.03E-10	2.62E-10	5.71E-11	7.96E-11	7.51E-12	1.40E-11
9983.906	3983.906	1.46E-10	2.03E-10	3.73E-11	5.90E-11	4.25E-12	1.08E-11
10350.47	4350.47	1.10E-10	1.67E-10	2.63E-11	4.87E-11	2.89E-12	9.53E-12
10717.03	4717.03	8.77E-11	1.45E-10	2.07E-11	4.35E-11	2.48E-12	8.88E-12
11083.59	5083.59	7.47E-11	1.33E-10	1.83E-11	4.10E-11	2.40E-12	8.48E-12
11450.16	5450.16	6.80E-11	1.26E-10	1.73E-11	3.97E-11	2.38E-12	8.24E-12

without oil_1 Hz	oil_1 Hz
1.28E-13	8.78E-13
1.31E-13	9.10E-13
1.33E-13	9.65E-13
1.31E-13	1.04E-12
1.55E-13	1.12E-12
3.28E-13	1.25E-12
8.66E-13	1.80E-12
2.43E-12	3.94E-12
7.59E-12	1.03E-11
2.59E-11	2.96E-11
9.22E-11	9.62E-11
3.38E-10	3.41E-10
1.26E-09	1.27E-09
4.83E-09	4.83E-09
1.92E-08	1.92E-08
1.14E-07	1.14E-07
1.14E-07	1.14E-07
1.92E-08	1.92E-08
4.83E-09	4.83E-09
1.26E-09	1.27E-09
3.38E-10	3.41E-10
9.22E-11	9.62E-11
2.59E-11	2.96E-11
7.59E-12	1.03E-11
2.43E-12	3.94E-12
8.66E-13	1.80E-12
3.28E-13	1.25E-12
1.55E-13	1.12E-12
1.31E-13	1.04E-12
1.33E-13	9.65E-13
1.31E-13	9.10E-13
1.28E-13	8.78E-13

APPENDIX F

Raw Reading for Simulation 4

Offset (0.5 Hz)	without oil	oil, ob_400	oil, ob_600	oil, ob_800	oil, ob_1000	oil, ob_1200	oil, ob_1400	oil, ob_1600	oil, ob_1800
-5816.7187	2.28E-12	5.49E-11	2.84E-11	1.33E-11	8.24E-12	5.36E-12	4.03E-12	2.97E-12	2.44E-12
-5450.1562	2.29E-12	5.70E-11	2.95E-11	1.37E-11	8.48E-12	5.50E-12	4.13E-12	3.04E-12	2.48E-12
-5083.5937	2.39E-12	6.05E-11	3.13E-11	1.45E-11	8.88E-12	5.78E-12	4.39E-12	3.25E-12	2.64E-12
-4717.031	2.82E-12	6.58E-11	3.40E-11	1.55E-11	9.53E-12	6.38E-12	5.04E-12	3.87E-12	3.20E-12
-4350.469	4.19E-12	7.32E-11	3.74E-11	1.69E-11	1.08E-11	7.86E-12	6.65E-12	5.42E-12	4.71E-12
-3983.906	7.39E-12	8.25E-11	4.16E-11	1.92E-11	1.40E-11	1.15E-11	1.03E-11	8.81E-12	8.02E-12
-3617.344	1.43E-11	9.34E-11	4.71E-11	2.53E-11	2.25E-11	1.97E-11	1.79E-11	1.58E-11	1.50E-11
-3250.781	3.01E-11	1.06E-10	6.00E-11	4.38E-11	4.25E-11	3.76E-11	3.44E-11	3.15E-11	3.07E-11
-2884.219	7.03E-11	1.33E-10	1.05E-10	9.28E-11	8.94E-11	8.00E-11	7.52E-11	7.14E-11	7.11E-11
-2517.656	1.80E-10	2.38E-10	2.35E-10	2.14E-10	2.06E-10	1.91E-10	1.85E-10	1.80E-10	1.81E-10
-2151.094	4.84E-10	5.77E-10	5.77E-10	5.29E-10	5.20E-10	4.96E-10	4.93E-10	4.83E-10	4.88E-10
-1784.531	1.35E-09	1.49E-09	1.48E-09	1.39E-09	1.41E-09	1.36E-09	1.37E-09	1.34E-09	1.36E-09
-1417.969	3.84E-09	3.99E-09	4.04E-09	3.88E-09	3.97E-09	3.86E-09	3.89E-09	3.82E-09	3.87E-09
-1051.406	1.12E-08	1.12E-08	1.16E-08	1.13E-08	1.16E-08	1.13E-08	1.13E-08	1.11E-08	1.13E-08
-684.844	3.42E-08	3.39E-08	3.57E-08	3.45E-08	3.54E-08	3.45E-08	3.46E-08	3.40E-08	3.45E-08
-342.422	1.42E-07	1.47E-07	1.51E-07	1.48E-07	1.50E-07	1.48E-07	1.43E-07	1.41E-07	1.43E-07
-24.141	1.42E-07	1.47E-07	1.51E-07	1.48E-07	1.50E-07	1.48E-07	1.43E-07	1.41E-07	1.43E-07
318.281	3.42E-08	3.39E-08	3.57E-08	3.45E-08	3.54E-08	3.45E-08	3.46E-08	3.40E-08	3.45E-08
684.844	1.12E-08	1.12E-08	1.16E-08	1.13E-08	1.16E-08	1.13E-08	1.13E-08	1.11E-08	1.13E-08
1051.406	3.84E-09	3.99E-09	4.04E-09	3.88E-09	3.97E-09	3.86E-09	3.89E-09	3.82E-09	3.87E-09
1417.969	1.35E-09	1.49E-09	1.48E-09	1.39E-09	1.41E-09	1.36E-09	1.37E-09	1.34E-09	1.36E-09
1784.531	4.84E-10	5.77E-10	5.77E-10	5.29E-10	5.20E-10	4.96E-10	4.93E-10	4.83E-10	4.88E-10
2151.094	1.80E-10	2.38E-10	2.35E-10	2.14E-10	2.06E-10	1.91E-10	1.85E-10	1.80E-10	1.81E-10
2517.656	7.03E-11	1.33E-10	1.05E-10	9.28E-11	8.94E-11	8.00E-11	7.52E-11	7.14E-11	7.11E-11
2884.219	3.01E-11	1.06E-10	6.00E-11	4.38E-11	4.25E-11	3.76E-11	3.44E-11	3.15E-11	3.07E-11
3250.781	1.43E-11	9.34E-11	4.71E-11	2.53E-11	2.25E-11	1.97E-11	1.79E-11	1.58E-11	1.50E-11
3617.344	7.39E-12	8.25E-11	4.16E-11	1.92E-11	1.40E-11	1.15E-11	1.03E-11	8.81E-12	8.02E-12
3983.906	4.19E-12	7.32E-11	3.74E-11	1.69E-11	1.08E-11	7.86E-12	6.65E-12	5.42E-12	4.71E-12
4350.47	2.82E-12	6.58E-11	3.40E-11	1.55E-11	9.53E-12	6.38E-12	5.04E-12	3.87E-12	3.20E-12
4717.03	2.39E-12	6.05E-11	3.13E-11	1.45E-11	8.88E-12	5.78E-12	4.39E-12	3.25E-12	2.64E-12
5083.59	2.29E-12	5.70E-11	2.95E-11	1.37E-11	8.48E-12	5.50E-12	4.13E-12	3.04E-12	2.48E-12
5450.16	2.28E-12	5.49E-11	2.84E-11	1.33E-11	8.24E-12	5.36E-12	4.03E-12	2.97E-12	2.44E-12

oil, ob_2000	oil, ob_2200	oil, ob_2400	oil, ob_2600		Offset (0.125 Hz)	without oil	oil, ob_400	oil, ob_600	oil, ob_800
2.20E-12	2.20E-12	2.22E-12	2.27E-12		-5816.7187	6.30E-11	1.69E-10	1.56E-10	1.34E-10
2.22E-12	2.21E-12	2.23E-12	2.28E-12		-5450.1562	6.90E-11	1.76E-10	1.63E-10	1.41E-10
2.22E-12	2.31E-12	2.32E-12	2.37E-12		-5083.5937	8.08E-11	1.76E-10	1.75E-10	1.53E-10
2.84E-12	2.76E-12	2.75E-12	2.80E-12		-4717.031	1.01E-10	2.09E-10	1.97E-10	1.74E-10
4.27E-12	4.15E-12	4.11E-12	4.16E-12		-4350.469	1.34E-10	2.45E-10	2.35E-10	2.09E-10
7.48E-12	7.38E-12	7.30E-12	7.38E-12		-3983.906	1.88E-10	3.08E-10	2.99E-10	2.68E-10
1.43E-11	1.43E-11	1.41E-11	1.43E-11		-3617.344	2.78E-10	4.19E-10	4.08E-10	3.67E-10
2.99E-11	3.02E-11	2.99E-11	3.02E-11		-3250.781	4.37E-10	6.16E-10	6.00E-10	5.39E-10
6.99E-11	7.06E-11	6.99E-11	7.06E-11		-2884.219	7.36E-10	9.74E-10	9.47E-10	8.50E-10
1.79E-10	1.81E-10	1.79E-10	1.80E-10		-2517.656	1.33E-09	1.65E-09	1.60E-09	1.45E-09
4.82E-10	4.87E-10	1.79E-10	4.86E-10		-2151.094	2.58E-09	2.97E-09	2.91E-09	2.67E-09
1.34E-09	1.36E-09	1.34E-09	1.35E-09		-1784.531	5.27E-09	5.68E-09	5.67E-09	5.30E-09
3.82E-09	3.86E-09	3.82E-09	3.86E-09		-1417.969	1.13E-08	1.16E-08	1.18E-08	1.12E-08
1.11E-08	1.13E-08	1.11E-08	1.13E-08		-1051.406	2.53E-08	2.51E-08	2.63E-08	2.52E-08
3.40E-08	3.44E-08	3.40E-08	3.44E-08		-684.844	6.06E-08	5.97E-08	6.30E-08	6.06E-08
1.41E-07	1.42E-07	1.41E-07	1.42E-07		-342.422	1.91E-07	1.95E-07	2.03E-07	1.97E-07
1.41E-07	1.42E-07	1.41E-07	1.42E-07		-24.141	1.91E-07	1.95E-07	2.03E-07	1.97E-07
3.40E-08	3.44E-08	3.40E-08	3.44E-08		318.281	6.06E-08	5.97E-08	6.30E-08	6.06E-08
1.11E-08	1.13E-08	1.11E-08	1.13E-08		684.844	2.53E-08	2.51E-08	2.63E-08	2.52E-08
3.82E-09	3.86E-09	3.82E-09	3.86E-09		1051.406	1.13E-08	1.16E-08	1.18E-08	1.12E-08
1.34E-09	1.36E-09	1.34E-09	1.35E-09		1417.969	5.27E-09	5.68E-09	5.67E-09	5.30E-09
4.82E-10	4.87E-10	4.82E-10	4.86E-10		1784.531	2.58E-09	2.97E-09	2.91E-09	2.67E-09
1.79E-10	1.81E-10	1.79E-10	1.80E-10		2151.094	1.33E-09	1.65E-09	1.60E-09	1.45E-09
6.99E-11	7.06E-11	6.99E-11	7.06E-11		2517.656	7.36E-10	9.74E-10	9.47E-10	8.50E-10
2.99E-11	3.02E-11	2.99E-11	3.02E-11		2884.219	4.37E-10	6.16E-10	6.00E-10	5.39E-10
1.43E-11	1.43E-11	1.41E-11	1.43E-11		3250.781	2.78E-10	4.19E-10	4.08E-10	3.67E-10
7.48E-12	7.38E-12	7.30E-12	7.38E-12		3617.344	1.88E-10	3.08E-10	2.99E-10	2.68E-10
4.27E-12	4.15E-12	4.11E-12	4.16E-12		3983.906	1.34E-10	2.45E-10	2.35E-10	2.09E-10
2.84E-12	2.76E-12	2.75E-12	2.80E-12		4350.47	1.01E-10	2.09E-10	1.97E-10	1.74E-10
2.35E-12	2.31E-12	2.32E-12	2.37E-12		4717.03	8.08E-11	1.88E-10	1.75E-10	1.53E-10
2.22E-12	2.21E-12	2.23E-12	2.28E-12		5083.59	6.90E-11	1.76E-10	1.63E-10	1.41E-10
2.20E-12	2.20E-12	2.22E-12	2.27E-12		5450.16	6.30E-11	1.69E-10	1.56E-10	1.34E-10

oil, ob_1000	oil, ob_1200	oil, ob_1400	oil, ob_1600	oil, ob_1800	oil, ob_2000	oil, ob_2200	oil, ob_2400	oil, ob_2600	
1.26E-10	1.10E-10	9.88E-11	8.65E-11	7.95E-11	7.17E-11	6.81E-11	6.42E-11	6.34E-11	
1.33E-10	1.17E-10	1.05E-10	9.28E-11	8.59E-11	7.80E-11	7.44E-11	7.05E-11	6.97E-11	
1.45E-10	1.29E-10	1.17E-10	1.05E-10	9.81E-11	9.00E-11	8.66E-11	8.25E-11	8.18E-11	
1.67E-10	1.49E-10	1.38E-10	1.25E-10	1.19E-10	1.10E-10	1.07E-10	1.03E-10	1.02E-10	
2.03E-10	1.83E-10	1.72E-10	1.58E-10	1.52E-10	1.43E-10	1.40E-10	1.36E-10	1.36E-10	
2.62E-10	2.38E-10	2.26E-10	2.10E-10	2.05E-10	1.95E-10	1.94E-10	1.89E-10	1.90E-10	
3.60E-10	3.30E-10	3.17E-10	2.97E-10	2.94E-10	2.83E-10	2.84E-10	2.78E-10	2.81E-10	
5.29E-10	4.88E-10	4.75E-10	4.52E-10	4.52E-10	4.39E-10	4.43E-10	4.35E-10	4.41E-10	
8.38E-10	7.82E-10	7.72E-10	7.43E-10	7.51E-10	7.34E-10	7.44E-10	7.32E-10	7.42E-10	
1.44E-09	1.37E-09	1.37E-09	1.33E-09	1.35E-09	1.32E-09	1.35E-09	1.32E-09	1.34E-09	
2.70E-09	2.59E-09	2.62E-09	2.56E-09	2.61E-09	2.56E-09	2.60E-09	2.56E-09	2.60E-09	
5.44E-09	5.26E-09	5.34E-09	5.22E-09	5.33E-09	5.23E-09	5.32E-09	5.24E-09	5.31E-09	
1.16E-08	1.13E-08	1.14E-08	1.12E-08	1.14E-08	1.12E-08	1.14E-08	1.12E-08	1.14E-08	
2.61E-08	2.53E-08	2.57E-08	2.52E-08	2.56E-08	2.52E-08	2.56E-08	2.52E-08	2.55E-08	
6.27E-08	6.09E-08	6.15E-08	6.02E-08	6.13E-08	6.02E-08	6.11E-08	6.02E-08	6.10E-08	
2.02E-07	1.98E-07	1.93E-07	1.90E-07	1.93E-07	1.90E-07	1.92E-07	1.90E-07	1.92E-07	
2.02E-07	1.98E-07	1.93E-07	1.90E-07	1.93E-07	1.90E-07	1.92E-07	1.90E-07	1.92E-07	
6.27E-08	6.09E-08	6.15E-08	6.02E-08	6.13E-08	6.02E-08	6.11E-08	6.02E-08	6.10E-08	
2.61E-08	2.53E-08	2.57E-08	2.52E-08	2.56E-08	2.52E-08	2.56E-08	2.52E-08	2.55E-08	
1.16E-08	1.13E-08	1.14E-08	1.12E-08	1.14E-08	1.12E-08	1.14E-08	1.12E-08	1.14E-08	
5.44E-09	5.26E-09	5.34E-09	5.22E-09	5.33E-09	5.23E-09	5.32E-09	5.24E-09	5.31E-09	
2.70E-09	2.59E-09	2.62E-09	2.56E-09	2.61E-09	2.56E-09	2.60E-09	2.56E-09	2.60E-09	
1.44E-09	1.37E-09	1.37E-09	1.33E-09	1.35E-09	1.32E-09	1.35E-09	1.32E-09	1.34E-09	
8.38E-10	7.82E-10	7.72E-10	7.43E-10	7.51E-10	7.34E-10	7.44E-10	7.32E-10	7.42E-10	
5.29E-10	4.88E-10	4.75E-10	4.52E-10	4.52E-10	4.39E-10	4.43E-10	4.35E-10	4.41E-10	
3.60E-10	3.30E-10	3.17E-10	2.97E-10	2.94E-10	2.83E-10	2.84E-10	2.78E-10	2.81E-10	
2.62E-10	2.38E-10	2.26E-10	2.10E-10	2.05E-10	1.95E-10	1.94E-10	1.89E-10	1.90E-10	
2.03E-10	1.83E-10	1.72E-10	1.58E-10	1.52E-10	1.43E-10	1.40E-10	1.36E-10	1.36E-10	
1.67E-10	1.49E-10	1.38E-10	1.25E-10	1.19E-10	1.10E-10	1.07E-10	1.03E-10	1.02E-10	
1.45E-10	1.29E-10	1.17E-10	1.05E-10	9.81E-11	9.00E-11	8.66E-11	8.25E-11	8.18E-11	
1.33E-10	1.17E-10	1.05E-10	9.28E-11	8.59E-11	7.80E-11	7.44E-11	7.05E-11	6.97E-11	
1.26E-10	1.10E-10	9.88E-11	8.65E-11	7.95E-11	7.17E-11	6.81E-11	6.42E-11	6.34E-11	

oil, ob_2000	oil, ob_2200	oil, ob_2400	oil, ob_2600		Offset (1 Hz)	without oil	oil, ob_400	oil, ob_600	oil, ob_800	oil, ob_1000
1.78E-11	1.69E-11	1.63E-11	1.65E-11		-5816.7187	1.22E-13	1.70E-11	6.55E-12	2.09E-12	8.78E-13
1.91E-11	1.81E-11	1.74E-11	1.75E-11		-5450.1562	1.25E-13	1.77E-11	6.80E-12	2.18E-12	9.10E-13
2.19E-11	2.08E-11	2.00E-11	2.01E-11		-5083.5937	1.26E-13	1.88E-11	7.25E-12	2.32E-12	9.65E-13
2.77E-11	2.66E-11	2.56E-11	2.56E-11		-4717.031	1.24E-13	2.06E-11	7.93E-12	2.53E-12	1.04E-12
3.84E-11	3.74E-11	3.62E-11	3.63E-11		-4350.469	1.50E-13	2.31E-11	8.88E-12	2.80E-12	1.12E-12
5.74E-11	5.67E-11	5.52E-11	5.56E-11		-3983.906	3.22E-13	2.65E-11	1.01E-11	3.10E-12	1.25E-12
9.19E-11	9.18E-11	8.99E-11	9.08E-11		-3617.344	8.47E-13	3.13E-11	1.17E-11	3.44E-12	1.80E-12
1.59E-10	1.60E-10	1.58E-10	1.59E-10		-3250.781	2.38E-12	3.73E-11	1.36E-11	4.81E-12	3.94E-12
3.03E-10	3.06E-10	3.01E-10	3.05E-10		-2884.219	7.45E-12	4.44E-11	1.85E-11	1.15E-11	1.03E-11
6.27E-10	6.35E-10	6.25E-10	6.33E-10		-2517.656	2.54E-11	5.84E-11	4.12E-11	3.35E-11	2.96E-11
1.38E-09	1.40E-09	1.38E-09	1.40E-09		-2151.094	9.06E-11	1.29E-10	1.20E-10	1.03E-10	9.62E-11
3.20E-09	3.24E-09	3.20E-09	3.23E-09		-1784.531	3.31E-10	4.05E-10	3.82E-10	3.48E-10	3.41E-10
7.65E-09	7.76E-09	7.65E-09	7.74E-09		-1417.969	1.24E-09	1.35E-09	1.32E-09	1.26E-09	1.27E-09
1.89E-08	1.92E-08	1.89E-08	1.91E-08		-1051.406	4.72E-09	4.82E-09	4.90E-09	4.76E-09	4.83E-09
4.94E-08	5.00E-08	4.93E-08	4.99E-08		-684.844	1.87E-08	1.88E-08	1.94E-08	1.89E-08	1.92E-08
1.71E-07	1.73E-07	1.71E-07	1.72E-07		-342.422	1.07E-07	1.13E-07	1.14E-07	1.13E-07	1.14E-07
1.71E-07	1.73E-07	1.71E-07	1.72E-07		-24.141	1.07E-07	1.13E-07	1.14E-07	1.13E-07	1.14E-07
4.94E-08	5.00E-08	4.93E-08	4.99E-08		318.281	1.87E-08	1.88E-08	1.94E-08	1.89E-08	1.92E-08
1.89E-08	1.92E-08	1.89E-08	1.91E-08		684.844	4.72E-09	4.82E-09	4.90E-09	4.76E-09	4.83E-09
7.65E-09	7.76E-09	7.65E-09	7.74E-09		1051.406	1.24E-09	1.35E-09	1.32E-09	1.26E-09	1.27E-09
3.20E-09	3.24E-09	3.20E-09	3.23E-09		1417.969	3.31E-10	4.05E-10	3.82E-10	3.48E-10	3.41E-10
1.38E-09	1.40E-09	1.38E-09	1.40E-09		1784.531	9.06E-11	1.29E-10	1.20E-10	1.03E-10	9.62E-11
6.27E-10	6.35E-10	6.25E-10	6.33E-10		2151.094	2.54E-11	5.84E-11	4.12E-11	3.35E-11	2.96E-11
3.03E-10	3.06E-10	3.01E-10	3.05E-10		2517.656	7.45E-12	4.44E-11	1.85E-11	1.15E-11	1.03E-11
1.59E-10	1.60E-10	1.58E-10	1.59E-10		2884.219	2.38E-12	3.73E-11	1.36E-11	4.81E-12	3.94E-12
9.19E-11	9.18E-11	8.99E-11	9.08E-11		3250.781	8.47E-13	3.13E-11	1.17E-11	3.44E-12	1.80E-12
5.74E-11	5.67E-11	5.52E-11	5.56E-11		3617.344	3.22E-13	2.65E-11	1.01E-11	3.10E-12	1.25E-12
3.84E-11	3.74E-11	3.62E-11	3.63E-11		3983.906	1.50E-13	2.31E-11	8.88E-12	2.80E-12	1.12E-12
2.77E-11	2.66E-11	2.56E-11	2.56E-11		4350.47	1.24E-13	2.06E-11	7.93E-12	2.53E-12	1.04E-12
2.19E-11	2.08E-11	2.00E-11	2.01E-11		4717.03	1.26E-13	1.88E-11	7.25E-12	2.32E-12	9.65E-13
1.91E-11	1.81E-11	1.74E-11	1.75E-11		5083.59	1.25E-13	1.77E-11	6.80E-12	2.18E-12	9.10E-13
1.78E-11	1.69E-11	1.63E-11	1.65E-11		5450.16	1.22E-13	1.70E-11	6.55E-12	2.09E-12	8.78E-13

oil, ob_1200	oil, ob_1400	oil, ob_1600	oil, ob_1800	oil, ob_2000	oil, ob_2200	oil, ob_2400	oil, ob_2600
3.83E-13	2.25E-13	1.41E-13	1.17E-13	1.17E-13	1.22E-13	1.21E-13	1.23E-13
3.96E-13	2.31E-13	1.43E-13	1.19E-13	1.19E-13	1.25E-13	1.24E-13	1.26E-13
4.14E-13	2.39E-13	1.46E-13	1.20E-13	1.20E-13	1.26E-13	1.25E-13	1.27E-13
4.35E-13	2.51E-13	1.50E-13	1.18E-13	1.18E-13	1.24E-13	1.23E-13	1.26E-13
4.70E-13	2.98E-13	1.90E-13	1.48E-13	1.44E-13	1.48E-13	1.49E-13	1.51E-13
6.37E-13	4.99E-13	3.77E-13	3.25E-13	3.17E-13	3.19E-13	3.21E-13	3.22E-13
1.29E-12	1.08E-12	9.07E-13	8.46E-13	8.37E-13	8.44E-13	8.44E-13	8.48E-13
3.13E-12	2.65E-12	2.42E-12	2.37E-12	2.36E-12	2.38E-12	2.37E-12	2.38E-12
8.52E-12	7.67E-12	7.42E-12	7.43E-12	7.42E-12	7.46E-12	7.43E-12	7.46E-12
2.66E-11	2.55E-11	2.53E-11	2.54E-11	2.53E-11	2.54E-11	2.53E-11	2.54E-11
9.19E-11	9.09E-11	9.03E-11	9.09E-11	9.04E-11	9.08E-11	9.04E-11	9.08E-11
3.34E-10	3.33E-10	3.30E-10	3.33E-10	3.30E-10	3.33E-10	3.31E-10	3.32E-10
1.24E-09	1.25E-09	1.23E-09	1.25E-09	1.23E-09	1.24E-09	1.23E-09	1.24E-09
4.74E-09	4.76E-09	4.70E-09	4.75E-09	4.70E-09	4.74E-09	4.70E-09	4.73E-09
1.89E-08	1.89E-08	1.86E-08	1.88E-08	1.86E-08	1.88E-08	1.86E-08	1.88E-08
1.13E-07	1.07E-07						
1.13E-07	1.07E-07						
1.89E-08	1.89E-08	1.86E-08	1.88E-08	1.86E-08	1.88E-08	1.86E-08	1.88E-08
4.74E-09	4.76E-09	4.70E-09	4.75E-09	4.70E-09	4.74E-09	4.70E-09	4.73E-09
1.24E-09	1.25E-09	1.23E-09	1.25E-09	1.23E-09	1.24E-09	1.23E-09	1.24E-09
3.34E-10	3.33E-10	3.30E-10	3.33E-10	3.30E-10	3.33E-10	3.31E-10	3.32E-10
9.19E-11	9.09E-11	9.03E-11	9.09E-11	9.04E-11	9.08E-11	9.04E-11	9.08E-11
2.66E-11	2.55E-11	2.53E-11	2.54E-11	2.53E-11	2.54E-11	2.53E-11	2.54E-11
8.52E-12	7.67E-12	7.42E-12	7.43E-12	7.42E-12	7.46E-12	7.43E-12	7.46E-12
3.13E-12	2.65E-12	2.42E-12	2.37E-12	2.36E-12	2.38E-12	2.37E-12	2.38E-12
1.29E-12	1.08E-12	9.07E-13	8.46E-13	8.37E-13	8.44E-13	8.44E-13	8.48E-13
6.37E-13	4.99E-13	3.77E-13	3.25E-13	3.17E-13	3.19E-13	3.21E-13	3.22E-13
4.70E-13	2.98E-13	1.90E-13	1.48E-13	1.44E-13	1.48E-13	1.49E-13	1.51E-13
4.35E-13	2.51E-13	1.50E-13	1.18E-13	1.18E-13	1.24E-13	1.23E-13	1.26E-13
4.14E-13	2.39E-13	1.46E-13	1.20E-13	1.20E-13	1.26E-13	1.25E-13	1.27E-13
3.96E-13	2.31E-13	1.43E-13	1.19E-13	1.19E-13	1.25E-13	1.24E-13	1.26E-13
3.83E-13	2.25E-13	1.41E-13	1.17E-13	1.17E-13	1.22E-13	1.21E-13	1.23E-13

APPENDIX G
Raw Reading for Simulation 5

Length		Offset, 0.78 MHz	without oil	oil		Offset, 1.56 MHz	without oil	oil		Offset, 3.13 MHz
7.28125		-232.71875	1.39E-15	2.09E-15		-232.71875	3.67E-16	5.29E-16		-232.71875
21.84375		-218.15625	1.39E-15	2.21E-15		-218.15625	3.81E-16	5.53E-16		-218.15625
36.40625		-203.59375	1.66E-15	2.41E-15		-203.59375	4.11E-16	5.98E-16		-203.59375
50.96875		-189.03125	1.87E-15	2.66E-15		-189.03125	4.63E-16	6.72E-16		-189.03125
65.53125		-174.46875	2.09E-15	2.93E-15		-174.46875	5.43E-16	7.79E-16		-174.46875
80.09375		-159.90625	2.29E-15	3.17E-15		-159.90625	6.41E-16	9.12E-16		-159.90625
94.65625		-145.34375	2.37E-15	3.29E-15		-145.34375	7.33E-16	1.04E-15		-145.34375
109.2187		-130.7813	2.18E-15	3.10E-15		-130.7813	7.56E-16	1.11E-15		-130.7813
123.7812		-116.2188	1.46E-15	2.37E-15		-116.2188	5.84E-16	9.77E-16		-116.2188
138.3437		-101.6563	7.10E-16	1.17E-15		-101.6563	1.50E-16	4.69E-16		-101.6563
152.9062		-87.0938	4.33E-15	4.11E-15		-87.0938	1.75E-15	1.51E-15		-87.0938
167.4687		-72.5313	1.22E-14	1.22E-14		-72.5313	5.79E-15	5.62E-15		-72.5313
182.0312		-57.9688	2.88E-14	2.92E-14		-57.9688	1.59E-14	1.59E-14		-57.9688
196.5937		-43.4063	6.83E-14	6.88E-14		-43.4063	4.43E-14	4.42E-14		-43.4063
211.1562		-28.8438	1.78E-13	1.78E-13		-28.8438	1.35E-13	1.35E-13		-28.8438
225.5781		-14.4219	4.86E-13	4.87E-13		-14.4219	4.13E-13	4.13E-13		-14.4219
239.8594		-0.1406	4.86E-13	4.87E-13		-0.1406	4.13E-13	4.13E-13		-0.1406
254.2813		14.2813	1.78E-13	1.78E-13		14.2813	1.35E-13	1.35E-13		14.2813
268.8438		28.8438	6.83E-14	6.88E-14		28.8438	4.43E-14	4.42E-14		28.8438
283.4063		43.4063	2.88E-14	2.92E-14		43.4063	1.59E-14	1.59E-14		43.4063
297.9688		57.9688	1.22E-14	1.22E-14		57.9688	5.79E-15	5.62E-15		57.9688
312.5313		72.5313	4.33E-15	4.11E-15		72.5313	1.75E-15	1.51E-15		72.5313
327.0938		87.0938	7.10E-16	1.17E-15		87.0938	1.50E-16	4.69E-16		87.0938
341.6563		101.6563	1.46E-15	2.37E-15		101.6563	5.84E-16	9.77E-16		101.6563
356.2188		116.2188	2.18E-15	3.10E-15		116.2188	7.56E-16	1.11E-15		116.2188
370.7813		130.7813	2.37E-15	3.29E-15		130.7813	7.33E-16	1.04E-15		130.7813
385.3438		145.3438	2.29E-15	3.17E-15		145.3438	6.41E-16	9.12E-16		145.3438
399.9063		159.9063	2.09E-15	2.93E-15		159.9063	5.43E-16	7.79E-16		159.9063
414.4688		174.4688	1.87E-15	2.66E-15		174.4688	4.63E-16	6.72E-16		174.4688
429.0313		189.0313	1.66E-15	2.41E-15		189.0313	4.11E-16	5.98E-16		189.0313
443.5938		203.5938	1.49E-15	2.21E-15		203.5938	3.81E-16	5.53E-16		203.5938
458.1563		218.1563	1.39E-15	2.09E-15		218.1563	3.67E-16	5.29E-16		218.1563

without oil	oil		Offset, 6.25 MHz	without oil	oil
5.70E-17	8.94E-17		-232.71875	3.39E-18	6.52E-18
5.83E-17	9.19E-17		-218.15625	3.49E-18	6.73E-18
6.07E-17	9.64E-17		-203.59375	3.66E-18	7.09E-18
6.52E-17	1.04E-16		-189.03125	3.90E-18	7.62E-18
7.39E-17	1.18E-16		-174.46875	4.24E-18	8.36E-18
8.95E-17	1.41E-16		-159.90625	4.88E-18	9.56E-18
1.11E-16	1.74E-16		-145.34375	6.21E-18	1.18E-17
1.31E-16	2.10E-16		-130.7813	8.25E-18	1.58E-17
1.18E-16	2.19E-16		-116.2188	9.11E-18	2.01E-17
3.75E-18	1.27E-16		-101.6563	2.24E-18	1.66E-17
4.23E-16	3.10E-16		-87.0938	4.33E-17	2.58E-17
1.73E-15	1.63E-15		-72.5313	2.53E-16	2.38E-16
6.02E-15	5.92E-15		-57.9688	1.32E-15	1.31E-15
2.17E-14	2.15E-14		-43.4063	7.03E-15	7.00E-15
8.35E-14	8.33E-14		-28.8438	3.70E-14	3.70E-14
2.99E-13	2.98E-13		-14.4219	1.63E-13	1.63E-13
2.99E-13	2.98E-13		-0.1406	1.63E-13	1.63E-13
8.35E-14	8.33E-14		14.2813	3.70E-14	3.70E-14
2.17E-14	2.15E-14		28.8438	7.03E-15	7.00E-15
6.02E-15	5.92E-15		43.4063	1.32E-15	1.31E-15
1.73E-15	1.63E-15		57.9688	2.53E-16	2.38E-16
4.23E-16	3.10E-16		72.5313	4.33E-17	2.58E-17
3.75E-18	1.27E-16		87.0938	2.24E-18	1.66E-17
1.18E-16	2.19E-16		101.6563	9.11E-18	2.01E-17
1.31E-16	2.10E-16		116.2188	8.25E-18	1.58E-17
1.11E-16	1.74E-16		130.7813	6.21E-18	1.18E-17
8.95E-17	1.41E-16		145.3438	4.88E-18	9.56E-18
7.39E-17	1.18E-16		159.9063	4.24E-18	8.36E-18
6.52E-17	1.04E-16		174.4688	3.90E-18	7.62E-18
6.07E-17	9.64E-17		189.0313	3.66E-18	7.09E-18
5.83E-17	9.19E-17		203.5938	3.49E-18	6.73E-18
5.70E-17	8.94E-17		218.1563	3.39E-18	6.52E-18

APPENDIX H
Raw Reading for Simulation 6.

Offset (0.78 MHz)	without oil	oil, ob_16	oil, ob_24	oil, ob_32	oil, ob_40	oil, ob_48	oil, ob_56	oil, ob_64	oil, ob_72	oil, ob_80
-232.71875	1.35E-15	2.62E-15	2.52E-15	2.23E-15	2.09E-15	1.84E-15	1.68E-15	1.52E-15	1.45E-15	1.37E-15
-218.15625	1.45E-15	2.77E-15	2.67E-15	2.36E-15	2.21E-15	1.95E-15	1.79E-15	1.62E-15	1.55E-15	1.47E-15
-203.59375	1.60E-15	3.03E-15	2.91E-15	2.57E-15	2.41E-15	2.13E-15	1.96E-15	1.78E-15	1.72E-15	1.63E-15
-189.03125	1.80E-15	3.37E-15	3.24E-15	2.83E-15	2.66E-15	2.35E-15	2.17E-15	1.99E-15	1.92E-15	1.84E-15
-174.46875	2.02E-15	3.77E-15	3.62E-15	3.13E-15	2.93E-15	2.58E-15	2.41E-15	2.21E-15	2.15E-15	2.06E-15
-159.90625	2.21E-15	4.20E-15	4.00E-15	3.40E-15	3.17E-15	2.77E-15	2.61E-15	2.39E-15	2.35E-15	2.25E-15
-145.34375	2.29E-15	4.57E-15	4.29E-15	3.55E-15	3.29E-15	2.83E-15	2.68E-15	2.46E-15	2.44E-15	2.33E-15
-130.7813	2.13E-15	4.76E-15	4.33E-15	3.42E-15	3.10E-15	2.61E-15	2.49E-15	2.27E-15	2.27E-15	2.16E-15
-116.2188	1.48E-15	4.58E-15	3.89E-15	2.75E-15	2.37E-15	1.85E-15	1.80E-15	1.59E-15	1.62E-15	1.51E-15
-101.6563	8.17E-16	3.95E-15	2.83E-15	1.55E-15	1.17E-15	8.91E-16	8.50E-16	8.07E-16	8.27E-16	8.07E-16
-87.0938	4.08E-15	4.67E-15	3.97E-15	3.99E-15	4.11E-15	4.25E-15	4.02E-15	4.06E-15	4.02E-15	4.04E-15
-72.5313	1.14E-14	1.16E-14	1.19E-14	1.20E-14	1.22E-14	1.20E-14	1.15E-14	1.14E-14	1.14E-14	1.14E-14
-57.9688	2.71E-14	2.92E-14	2.99E-14	2.91E-14	2.92E-14	2.85E-14	2.74E-14	2.70E-14	2.72E-14	2.70E-14
-43.4063	6.36E-14	7.13E-14	7.18E-14	6.87E-14	6.88E-14	6.71E-14	6.43E-14	6.34E-14	6.40E-14	6.34E-14
-28.8438	1.61E-13	1.84E-13	1.85E-13	1.76E-13	1.78E-13	1.74E-13	1.64E-13	1.61E-13	1.63E-13	1.61E-13
-14.4219	4.21E-13	4.84E-13	5.02E-13	4.71E-13	4.87E-13	4.68E-13	4.32E-13	4.21E-13	4.30E-13	4.21E-13
-0.1406	4.21E-13	4.84E-13	5.02E-13	4.71E-13	4.87E-13	4.68E-13	4.32E-13	4.21E-13	4.30E-13	4.21E-13
14.2813	1.61E-13	1.84E-13	1.85E-13	1.76E-13	1.78E-13	1.74E-13	1.64E-13	1.61E-13	1.63E-13	1.61E-13
28.8438	6.36E-14	7.13E-14	7.18E-14	6.87E-14	6.88E-14	6.71E-14	6.43E-14	6.34E-14	6.40E-14	6.34E-14
43.4063	2.71E-14	2.92E-14	2.99E-14	2.91E-14	2.92E-14	2.85E-14	2.74E-14	2.70E-14	2.72E-14	2.70E-14
57.9688	1.14E-14	1.16E-14	1.19E-14	1.20E-14	1.22E-14	1.20E-14	1.15E-14	1.14E-14	1.14E-14	1.14E-14
72.5313	4.08E-15	4.67E-15	3.97E-15	3.99E-15	4.11E-15	4.25E-15	4.02E-15	4.06E-15	4.02E-15	4.04E-15
87.0938	8.17E-16	3.95E-15	2.83E-15	1.55E-15	1.17E-15	8.91E-16	8.50E-16	8.07E-16	8.27E-16	8.07E-16
101.6563	1.48E-15	4.58E-15	3.89E-15	2.75E-15	2.37E-15	1.85E-15	1.80E-15	1.59E-15	1.62E-15	1.51E-15
116.2188	2.13E-15	4.76E-15	4.33E-15	3.42E-15	3.10E-15	2.61E-15	2.49E-15	2.27E-15	2.27E-15	2.16E-15
130.7813	2.29E-15	4.57E-15	4.29E-15	3.55E-15	3.29E-15	2.83E-15	2.68E-15	2.46E-15	2.44E-15	2.33E-15
145.3438	2.21E-15	4.20E-15	4.00E-15	3.40E-15	3.17E-15	2.77E-15	2.61E-15	2.39E-15	2.35E-15	2.25E-15
159.9063	2.02E-15	3.77E-15	3.62E-15	3.13E-15	2.93E-15	2.58E-15	2.41E-15	2.21E-15	2.15E-15	2.06E-15
174.4688	1.80E-15	3.37E-15	3.24E-15	2.83E-15	2.66E-15	2.35E-15	2.17E-15	1.99E-15	1.92E-15	1.84E-15
189.0313	1.60E-15	3.03E-15	2.91E-15	2.57E-15	2.41E-15	2.13E-15	1.96E-15	1.78E-15	1.72E-15	1.63E-15
203.5938	1.45E-15	2.77E-15	2.67E-15	2.36E-15	2.21E-15	1.95E-15	1.79E-15	1.62E-15	1.55E-15	1.47E-15
218.1563	1.35E-15	2.62E-15	2.52E-15	2.23E-15	2.09E-15	1.84E-15	1.68E-15	1.52E-15	1.45E-15	1.37E-15

oil, ob_88	oil, ob_96		Offset (1.56 MHz)	without oil	oil, ob_16	oil, ob_24	oil, ob_32	oil, ob_40	oil, ob_48	oil, ob_56	oil, ob_64
1.35E-15	1.33E-15		-232.71875	3.59E-16	6.06E-16	6.12E-16	5.57E-16	5.29E-16	4.62E-16	4.18E-16	3.80E-16
1.46E-15	1.43E-15		-218.15625	3.74E-16	6.25E-16	6.33E-16	5.80E-16	5.53E-16	4.84E-16	4.38E-16	3.98E-16
1.62E-15	1.59E-15		-203.59375	4.05E-16	6.64E-16	6.78E-16	6.25E-16	5.98E-16	5.26E-16	4.77E-16	4.34E-16
1.83E-15	1.79E-15		-189.03125	4.57E-16	7.37E-16	7.57E-16	7.01E-16	6.72E-16	5.94E-16	5.41E-16	4.93E-16
2.06E-15	2.01E-15		-174.46875	5.35E-16	8.62E-16	8.82E-16	8.12E-16	7.79E-16	6.89E-16	6.32E-16	5.78E-16
2.26E-15	2.21E-15		-159.90625	6.32E-16	1.06E-15	1.06E-15	9.56E-16	9.12E-16	8.02E-16	7.42E-16	6.79E-16
2.36E-15	2.30E-15		-145.34375	7.21E-16	1.33E-15	1.28E-15	1.11E-15	1.04E-15	9.04E-16	8.44E-16	7.71E-16
2.20E-15	2.14E-15		-130.7813	7.45E-16	1.67E-15	1.51E-15	1.21E-15	1.11E-15	9.32E-16	8.78E-16	7.95E-16
1.57E-15	1.50E-15		-116.2188	5.82E-16	2.04E-15	1.64E-15	1.14E-15	9.77E-16	7.56E-16	7.19E-16	6.28E-16
8.17E-16	8.00E-16		-101.6563	1.17E-16	2.38E-15	1.55E-15	7.61E-16	4.69E-16	2.10E-16	1.75E-16	1.08E-16
4.01E-15	4.04E-15		-87.0938	1.63E-15	2.99E-15	1.88E-15	1.53E-15	1.51E-15	1.64E-15	1.53E-15	1.59E-15
1.14E-14	1.14E-14		-72.5313	5.48E-15	5.92E-15	5.52E-15	5.60E-15	5.62E-15	5.67E-15	5.40E-15	5.43E-15
2.72E-14	2.70E-14		-57.9688	1.50E-14	1.61E-14	1.62E-14	1.59E-14	1.59E-14	1.57E-14	1.50E-14	1.50E-14
6.40E-14	6.35E-14		-43.4063	4.12E-14	4.63E-14	4.59E-14	4.43E-14	4.42E-14	4.36E-14	4.14E-14	4.11E-14
1.63E-13	1.61E-13		-28.8438	1.22E-13	1.39E-13	1.39E-13	1.33E-13	1.35E-13	1.32E-13	1.23E-13	1.22E-13
4.28E-13	4.21E-13		-14.4219	3.55E-13	4.09E-13	4.24E-13	3.99E-13	4.13E-13	3.98E-13	3.64E-13	3.55E-13
4.28E-13	4.21E-13		-0.1406	3.55E-13	4.09E-13	4.24E-13	3.99E-13	4.13E-13	3.98E-13	3.64E-13	3.55E-13
1.63E-13	1.61E-13		14.2813	1.22E-13	1.39E-13	1.39E-13	1.33E-13	1.35E-13	1.32E-13	1.23E-13	1.22E-13
6.40E-14	6.35E-14		28.8438	4.12E-14	4.63E-14	4.59E-14	4.43E-14	4.42E-14	4.36E-14	4.14E-14	4.11E-14
2.72E-14	2.70E-14		43.4063	1.50E-14	1.61E-14	1.62E-14	1.59E-14	1.59E-14	1.57E-14	1.50E-14	1.50E-14
1.14E-14	1.14E-14		57.9688	5.48E-15	5.92E-15	5.52E-15	5.60E-15	5.62E-15	5.67E-15	5.40E-15	5.43E-15
4.01E-15	4.04E-15		72.5313	1.63E-15	2.99E-15	1.88E-15	1.53E-15	1.51E-15	1.64E-15	1.53E-15	1.59E-15
8.17E-16	8.00E-16		87.0938	1.17E-16	2.38E-15	1.55E-15	7.61E-16	4.69E-16	2.10E-16	1.75E-16	1.08E-16
1.57E-15	1.50E-15		101.6563	5.82E-16	2.04E-15	1.64E-15	1.14E-15	9.77E-16	7.56E-16	7.19E-16	6.28E-16
2.20E-15	2.14E-15		116.2188	7.45E-16	1.67E-15	1.51E-15	1.21E-15	1.11E-15	9.32E-16	8.78E-16	7.95E-16
2.36E-15	2.30E-15		130.7813	7.21E-16	1.33E-15	1.28E-15	1.11E-15	1.04E-15	9.04E-16	8.44E-16	7.71E-16
2.26E-15	2.21E-15		145.3438	6.32E-16	1.06E-15	1.06E-15	9.56E-16	9.12E-16	8.02E-16	7.42E-16	6.79E-16
2.06E-15	2.01E-15		159.9063	5.35E-16	8.62E-16	8.82E-16	8.12E-16	7.79E-16	6.89E-16	6.32E-16	5.78E-16
1.83E-15	1.79E-15		174.4688	4.57E-16	7.37E-16	7.57E-16	7.01E-16	6.72E-16	5.94E-16	5.41E-16	4.93E-16
1.62E-15	1.59E-15		189.0313	4.05E-16	6.64E-16	6.78E-16	6.25E-16	5.98E-16	5.26E-16	4.77E-16	4.34E-16
1.46E-15	1.43E-15		203.5938	3.74E-16	6.25E-16	6.33E-16	5.80E-16	5.53E-16	4.84E-16	4.38E-16	3.98E-16
1.35E-15	1.33E-15		218.1563	3.59E-16	6.06E-16	6.12E-16	5.57E-16	5.29E-16	4.62E-16	4.18E-16	3.80E-16

oil_ob_72	oil_ob_80	oil_ob_88	oil_ob_96		Offset (3.13 MHz)	without oil	oil_ob_16	oil_ob_24	oil_ob_32	oil_ob_40	oil_ob_48
3.65E-16	3.54E-16	3.55E-16	3.54E-16		-232.71875	5.58E-17	2.53E-16	1.44E-16	9.72E-17	8.94E-17	7.36E-17
3.82E-16	3.70E-16	3.71E-16	3.68E-16		-218.15625	5.71E-17	2.62E-16	1.49E-16	9.99E-17	9.19E-17	7.56E-17
4.16E-16	4.02E-16	4.02E-16	3.99E-16		-203.59375	5.95E-17	2.77E-16	1.57E-16	1.05E-16	9.64E-17	7.94E-17
4.74E-16	4.57E-16	4.57E-16	4.53E-16		-189.03125	6.40E-17	3.00E-16	1.69E-16	1.13E-16	1.04E-16	8.62E-17
5.58E-16	5.38E-16	5.38E-16	5.31E-16		-174.46875	7.25E-17	3.31E-16	1.86E-16	1.26E-16	1.18E-16	9.83E-17
6.61E-16	6.36E-16	6.38E-16	6.28E-16		-159.90625	8.74E-17	3.76E-16	2.15E-16	1.50E-16	1.41E-16	1.18E-16
7.57E-16	7.26E-16	7.33E-16	7.18E-16		-145.34375	1.08E-16	4.49E-16	2.67E-16	1.87E-16	1.74E-16	1.45E-16
7.88E-16	7.51E-16	7.64E-16	7.43E-16		-130.7813	1.26E-16	5.77E-16	3.54E-16	2.37E-16	2.10E-16	1.69E-16
6.32E-16	5.89E-16	6.09E-16	5.81E-16		-116.2188	1.12E-16	7.98E-16	4.77E-16	2.76E-16	2.19E-16	1.59E-16
1.24E-16	1.07E-16	1.21E-16	1.12E-16		-101.6563	1.47E-17	1.13E-15	6.06E-16	2.51E-16	1.27E-16	3.74E-17
1.58E-15	1.62E-15	1.60E-15	1.63E-15		-87.0938	4.16E-16	1.54E-15	7.13E-16	3.31E-16	3.10E-16	3.93E-16
5.43E-15	5.46E-15	5.46E-15	5.48E-15		-72.5313	1.68E-15	2.24E-15	1.53E-15	1.58E-15	1.63E-15	1.72E-15
1.50E-14	1.50E-14	1.51E-14	1.50E-14		-57.9688	5.75E-15	5.98E-15	5.80E-15	5.92E-15	5.92E-15	6.00E-15
4.14E-14	4.12E-14	4.14E-14	4.12E-14		-43.4063	2.02E-14	2.24E-14	2.18E-14	2.16E-14	2.15E-14	2.16E-14
1.23E-13	1.22E-13	1.23E-13	1.22E-13		-28.8438	7.45E-14	8.53E-14	8.45E-14	8.20E-14	8.33E-14	8.21E-14
3.62E-13	3.55E-13	3.61E-13	3.55E-13		-14.4219	2.53E-13	2.93E-13	3.04E-13	2.87E-13	2.98E-13	2.88E-13
3.62E-13	3.55E-13	3.61E-13	3.55E-13		-0.1406	2.53E-13	2.93E-13	3.04E-13	2.87E-13	2.98E-13	2.88E-13
1.23E-13	1.22E-13	1.23E-13	1.22E-13		14.2813	7.45E-14	8.53E-14	8.45E-14	8.20E-14	8.33E-14	8.21E-14
4.14E-14	4.12E-14	4.14E-14	4.12E-14		28.8438	2.02E-14	2.24E-14	2.18E-14	2.16E-14	2.15E-14	2.16E-14
1.50E-14	1.50E-14	1.51E-14	1.50E-14		43.4063	5.75E-15	5.98E-15	5.80E-15	5.92E-15	5.92E-15	6.00E-15
5.43E-15	5.46E-15	5.46E-15	5.48E-15		57.9688	1.68E-15	2.24E-15	1.53E-15	1.58E-15	1.63E-15	1.72E-15
1.58E-15	1.62E-15	1.60E-15	1.63E-15		72.5313	4.16E-16	1.54E-15	7.13E-16	3.31E-16	3.10E-16	3.93E-16
1.24E-16	1.07E-16	1.21E-16	1.12E-16		87.0938	1.47E-17	1.13E-15	6.06E-16	2.51E-16	1.27E-16	3.74E-17
6.32E-16	5.89E-16	6.09E-16	5.81E-16		101.6563	1.12E-16	7.98E-16	4.77E-16	2.76E-16	2.19E-16	1.59E-16
7.88E-16	7.51E-16	7.64E-16	7.43E-16		116.2188	1.26E-16	5.77E-16	3.54E-16	2.37E-16	2.10E-16	1.69E-16
7.57E-16	7.26E-16	7.33E-16	7.18E-16		130.7813	1.08E-16	4.49E-16	2.67E-16	1.87E-16	1.74E-16	1.45E-16
6.61E-16	6.36E-16	6.38E-16	6.28E-16		145.3438	8.74E-17	3.76E-16	2.15E-16	1.50E-16	1.41E-16	1.18E-16
5.58E-16	5.38E-16	5.38E-16	5.31E-16		159.9063	7.25E-17	3.31E-16	1.86E-16	1.26E-16	1.18E-16	9.83E-17
4.74E-16	4.57E-16	4.57E-16	4.53E-16		174.4688	6.40E-17	3.00E-16	1.69E-16	1.13E-16	1.04E-16	8.62E-17
4.16E-16	4.02E-16	4.02E-16	3.99E-16		189.0313	5.95E-17	2.77E-16	1.57E-16	1.05E-16	9.64E-17	7.94E-17
3.82E-16	3.70E-16	3.71E-16	3.68E-16		203.5938	5.71E-17	2.62E-16	1.49E-16	9.99E-17	9.19E-17	7.56E-17
3.65E-16	3.54E-16	3.55E-16	3.54E-16		218.1563	5.58E-17	2.53E-16	1.44E-16	9.72E-17	8.94E-17	7.36E-17

oil, ob_56	oil, ob_64	oil, ob_72	oil, ob_80	oil, ob_88	oil, ob_96		Offset (6.25 MHz)	without oil	oil, ob_16	oil, ob_24	oil, ob_32
6.41E-17	5.74E-17	5.57E-17	5.50E-17	5.58E-17	5.56E-17		-232.71875	3.31E-18	6.52E-18	2.79E-17	9.21E-18
6.57E-17	5.88E-17	5.70E-17	5.62E-17	5.71E-17	5.69E-17		-218.15625	3.41E-18	6.73E-18	2.89E-17	9.53E-18
6.89E-17	6.15E-17	5.94E-17	5.86E-17	5.94E-17	5.93E-17		-203.59375	3.57E-18	7.09E-18	3.08E-17	1.01E-17
7.46E-17	6.65E-17	6.40E-17	6.30E-17	6.38E-17	6.37E-17		-189.03125	3.81E-18	7.62E-18	3.35E-17	1.09E-17
8.53E-17	7.59E-17	7.29E-17	7.15E-17	7.23E-17	7.21E-17		-174.46875	4.15E-18	8.36E-18	3.74E-17	1.21E-17
1.03E-16	9.21E-17	8.86E-17	8.65E-17	8.74E-17	8.70E-17		-159.90625	4.76E-18	9.56E-18	4.26E-17	1.37E-17
1.28E-16	1.14E-16	1.11E-16	1.07E-16	1.09E-16	1.08E-16		-145.34375	5.97E-18	1.18E-17	4.99E-17	1.63E-17
1.50E-16	1.33E-16	1.30E-16	1.25E-16	1.28E-16	1.25E-16		-130.7813	7.76E-18	1.58E-17	6.18E-17	2.17E-17
1.41E-16	1.20E-16	1.19E-16	1.12E-16	1.16E-16	1.12E-16		-116.2188	8.30E-18	2.01E-17	8.40E-17	3.08E-17
3.21E-17	2.09E-17	1.43E-17	1.65E-17	1.07E-17	1.50E-17		-101.6563	4.05E-18	1.66E-17	1.20E-16	3.82E-17
3.80E-16	4.10E-16	4.01E-16	4.16E-16	4.05E-16	4.16E-16		-87.0938	4.62E-17	2.58E-17	1.51E-16	2.30E-17
1.64E-15	1.67E-15	1.66E-15	1.68E-15	1.67E-15	1.68E-15		-72.5313	2.54E-16	2.38E-16	1.52E-16	2.07E-16
5.69E-15	5.74E-15	5.72E-15	5.75E-15	5.73E-15	5.75E-15		-57.9688	1.28E-15	1.31E-15	1.13E-15	1.31E-15
2.01E-14	2.01E-14	2.02E-14	2.02E-14	2.02E-14	2.02E-14		-43.4063	6.49E-15	7.00E-15	6.83E-15	7.06E-15
7.52E-14	7.45E-14	7.51E-14	7.45E-14	7.50E-14	7.45E-14		-28.8438	3.25E-14	3.70E-14	3.69E-14	3.65E-14
2.60E-13	2.53E-13	2.59E-13	2.53E-13	2.58E-13	2.53E-13		-14.4219	1.36E-13	1.63E-13	1.65E-13	1.57E-13
2.60E-13	2.53E-13	2.59E-13	2.53E-13	2.58E-13	2.53E-13		-0.1406	1.36E-13	1.63E-13	1.65E-13	1.57E-13
7.52E-14	7.45E-14	7.51E-14	7.45E-14	7.50E-14	7.45E-14		14.2813	3.25E-14	3.70E-14	3.69E-14	3.65E-14
2.01E-14	2.01E-14	2.02E-14	2.02E-14	2.02E-14	2.02E-14		28.8438	6.49E-15	7.00E-15	6.83E-15	7.06E-15
5.69E-15	5.74E-15	5.72E-15	5.75E-15	5.73E-15	5.75E-15		43.4063	1.28E-15	1.31E-15	1.13E-15	1.31E-15
1.64E-15	1.67E-15	1.66E-15	1.68E-15	1.67E-15	1.68E-15		57.9688	2.54E-16	2.38E-16	1.52E-16	2.07E-16
3.80E-16	4.10E-16	4.01E-16	4.16E-16	4.05E-16	4.16E-16		72.5313	4.62E-17	2.58E-17	1.51E-16	2.30E-17
3.21E-17	2.09E-17	1.43E-17	1.65E-17	1.07E-17	1.50E-17		87.0938	4.05E-18	1.66E-17	1.20E-16	3.82E-17
1.41E-16	1.20E-16	1.19E-16	1.12E-16	1.16E-16	1.12E-16		101.6563	8.30E-18	2.01E-17	8.40E-17	3.08E-17
1.50E-16	1.33E-16	1.30E-16	1.25E-16	1.28E-16	1.25E-16		116.2188	7.76E-18	1.58E-17	6.18E-17	2.17E-17
1.28E-16	1.14E-16	1.11E-16	1.07E-16	1.09E-16	1.08E-16		130.7813	5.97E-18	1.18E-17	4.99E-17	1.63E-17
1.03E-16	9.21E-17	8.86E-17	8.65E-17	8.74E-17	8.70E-17		145.3438	4.76E-18	9.56E-18	4.26E-17	1.37E-17
8.53E-17	7.59E-17	7.29E-17	7.15E-17	7.23E-17	7.21E-17		159.9063	4.15E-18	8.36E-18	3.74E-17	1.21E-17
7.46E-17	6.65E-17	6.40E-17	6.30E-17	6.38E-17	6.37E-17		174.4688	3.81E-18	7.62E-18	3.35E-17	1.09E-17
6.89E-17	6.15E-17	5.94E-17	5.86E-17	5.94E-17	5.93E-17		189.0313	3.57E-18	7.09E-18	3.08E-17	1.01E-17
6.57E-17	5.88E-17	5.70E-17	5.62E-17	5.71E-17	5.69E-17		203.5938	3.41E-18	6.73E-18	2.89E-17	9.53E-18
6.41E-17	5.74E-17	5.57E-17	5.50E-17	5.58E-17	5.56E-17		218.1563	3.31E-18	6.52E-18	2.79E-17	9.21E-18

oil, ob_40	oil, ob_48	oil, ob_56	oil, ob_64	oil, ob_72	oil, ob_80	oil, ob_88	oil, ob_96
6.52E-18	4.56E-18	3.67E-18	3.31E-18	3.30E-18	3.29E-18	3.35E-18	3.31E-18
6.73E-18	4.70E-18	3.78E-18	3.41E-18	3.40E-18	3.39E-18	3.45E-18	3.41E-18
7.09E-18	4.94E-18	3.97E-18	3.57E-18	3.57E-18	3.55E-18	3.62E-18	3.58E-18
7.62E-18	5.29E-18	4.24E-18	3.80E-18	3.80E-18	3.79E-18	3.85E-18	3.81E-18
8.36E-18	5.81E-18	4.64E-18	4.15E-18	4.13E-18	4.12E-18	4.19E-18	4.15E-18
9.56E-18	6.72E-18	5.37E-18	4.77E-18	4.73E-18	4.73E-18	4.80E-18	4.76E-18
1.18E-17	8.46E-18	6.80E-18	6.01E-18	5.97E-18	5.93E-18	6.04E-18	5.97E-18
1.58E-17	1.11E-17	8.94E-18	7.84E-18	7.85E-18	7.70E-18	7.91E-18	7.76E-18
2.01E-17	1.25E-17	9.95E-18	8.40E-18	8.60E-18	8.24E-18	8.63E-18	8.30E-18
1.66E-17	6.52E-18	5.19E-18	4.62E-18	3.57E-18	4.05E-18	3.56E-18	4.04E-18
2.58E-17	4.42E-17	4.35E-17	4.66E-17	4.40E-17	4.63E-17	4.42E-17	4.62E-17
2.38E-16	2.63E-16	2.47E-16	2.55E-16	2.48E-16	2.54E-16	2.49E-16	2.54E-16
1.31E-15	1.36E-15	1.25E-15	1.28E-15	1.25E-15	1.28E-15	1.26E-15	1.28E-15
7.00E-15	7.12E-15	6.42E-15	6.49E-15	6.43E-15	6.49E-15	6.44E-15	6.49E-15
3.70E-14	3.66E-14	3.27E-14	3.25E-14	3.27E-14	3.25E-14	3.26E-14	3.25E-14
1.63E-13	1.57E-13	1.40E-13	1.36E-13	1.39E-13	1.36E-13	1.39E-13	1.36E-13
1.63E-13	1.57E-13	1.40E-13	1.36E-13	1.39E-13	1.36E-13	1.39E-13	1.36E-13
3.70E-14	3.66E-14	3.27E-14	3.25E-14	3.27E-14	3.25E-14	3.26E-14	3.25E-14
7.00E-15	7.12E-15	6.42E-15	6.49E-15	6.43E-15	6.49E-15	6.44E-15	6.49E-15
1.31E-15	1.36E-15	1.25E-15	1.28E-15	1.25E-15	1.28E-15	1.26E-15	1.28E-15
2.38E-16	2.63E-16	2.47E-16	2.55E-16	2.48E-16	2.54E-16	2.49E-16	2.54E-16